MicroRNA156: A Potential Graft-Transmissible MicroRNA That Modulates Plant Architecture and Tuberization in *Solanum tuberosum* ssp. *andigena*[1][C][W][OPEN]

Sneha Bhogale, Ameya S. Mahajan, Bhavani Natarajan, Mohit Rajabhoj, Hirekodathakallu V. Thulasiram, and Anjan K. Banerjee*

Indian Institute of Science Education and Research, Biology Division, Pune 411008, Maharashtra, India (S.B., A.S.M., B.N., M.R., A.K.B.); and Council of Scientific and Industrial Research-National Chemical Laboratory, Chemical Biology Unit, Division of Organic Chemistry, Pune 411008, Maharashtra, India (H.V.T.)

MicroRNA156 (*miR156*) functions in maintaining the juvenile phase in plants. However, the mobility of this microRNA has not been demonstrated. So far, only three microRNAs, *miR399*, *miR395*, and *miR172*, have been shown to be mobile. We demonstrate here that *miR156* is a potential graft-transmissible signal that affects plant architecture and tuberization in potato (*Solanum tuberosum*). Under tuber-noninductive (long-day) conditions, *miR156* shows higher abundance in leaves and stems, whereas an increase in abundance of *miR156* has been observed in stolons under tuber-inductive (short-day) conditions, indicative of a photoperiodic control. Detection of *miR156* in phloem cells of wild-type plants and mobility assays in heterografts suggest that *miR156* is a graft-transmissible signal. This movement was correlated with changes in leaf morphology and longer trichomes in leaves. Overexpression of *miR156* in potato caused a drastic phenotype resulting in altered plant architecture and reduced tuber yield. *miR156* overexpression plants also exhibited altered levels of cytokinin and strigolactone along with increased levels of LONELY GUY1 and StCyclin D3.1 transcripts as compared with wild-type plants. RNA ligase-mediated rapid amplification of complementary DNA ends analysis validated SQUAMOSA PROMOTER BINDING-LIKE3 (StSPL3), StSPL6, StSPL9, StSPL13, and StLIGULELESS1 as targets of *miR156*. Gel-shift assays indicate the regulation of *miR172* by *miR156* through StSPL9. *miR156*-resistant SPL9 overexpression lines exhibited increased *miR172* levels under a short-day photoperiod, supporting *miR172* regulation via the *miR156*-SPL9 module. Overall, our results strongly suggest that *miR156* is a phloem-mobile signal regulating potato development.

Long-distance transport of signaling molecules is known to be a major component in regulating plant growth and development as well as their adaptation to changing environmental conditions. This transport is implemented by the plant's vascular system, especially through the complex of companion cells and sieve elements present in the phloem. Recent evidence has established the movement of macromolecules like proteins, mRNAs, and microRNAs (miRNAs) through the phloem. It is now clear that these entities act as long-distance signals for development and stress response pathways (Kehr and Buhtz, 2008; Atkins et al., 2011). A well-established example is the movement of FLOWERING TIME protein from leaves to the shoot apex in Arabidopsis (*Arabidopsis thaliana*) as a long-distance signal for the regulation of flowering time (Corbesier et al., 2007). Similarly, the movement of transcripts such as *GIBBERELLIC ACID INSENSITIVE* (Haywood et al., 2005), *BELL1 LIKE TRANSCRIPTION FACTOR5* (Banerjee et al., 2006a; Lin et al., 2013), *TOMATO KNOTTED2* (Kim et al., 2001), and *POTATO HOMEOBOX1 TRANSCRIPTION FACTOR* (Mahajan et al., 2012), acting as long-distance signals for plant developmental processes such as leaf development, tuberization, and root growth, has been demonstrated. The movement of small interfering RNAs is also reported in a few cases where the induction of posttranscriptional gene silencing against viruses has been well studied (Waterhouse et al., 2001). In addition, small interfering RNAs were also demonstrated to be mobile and to exert epigenetic changes in recipient cells (Molnar et al., 2010). However, very limited information is available on the mobility of plant miRNAs, another group of small noncoding RNAs. Recent reviews have summarized the miRNAs found in phloem exudates of different plant species, but little information is available on their mobility (Kehr and Buhtz, 2008, 2013; Chuck and O'Connor, 2010).

The cellular movement of *microRNA165/166* (*miR165/166*) in root patterning, where mature *miR165/166* appears

[1] This work was supported by the Indian Institute of Science Education and Research, the Council of Scientific and Industrial Research, India, and the Department of Biotechnology, India.

* Address correspondence to akb@iiserpune.ac.in.

The author responsible for distribution of materials integral to the findings presented in this article in accordance with the policy described in the Instructions for Authors (www.plantphysiol.org) is: Anjan Kumar Banerjee (akb@iiserpune.ac.in).

[C] Some figures in this article are displayed in color online but in black and white in the print edition.

[W] The online version of this article contains Web-only data.

[OPEN] Articles can be viewed online without a subscription.

www.plantphysiol.org/cgi/doi/10.1104/pp.113.230714

to move from its site of biogenesis to adjacent cell layers, is an example of the short-distance movement of miRNA (Carlsbecker et al., 2010; Miyashima et al., 2011). Although some reports (Yoo et al., 2004; Buhtz et al., 2008; Varkonyi-Gasic et al., 2010) have demonstrated the presence of numerous miRNAs in phloem tissues, so far, only three miRNAs (*miR399*, *miR395*, and *miR172*) have been shown to move long distance in plants. *miR399* acts as a long-distance mobile signal that regulates phosphate homeostasis in Arabidopsis (Pant et al., 2008), whereas *miR395* was shown to move from wild-type scions to rootstocks of the miRNA-processing mutant *hen1-1* under sulfate stress (Buhtz et al., 2010). In another study, Martin and coworkers (2009) proposed that *miR172* functions as a long-distance mobile signal for potato (*Solanum tuberosum*) tuberization. Later, Kasai et al. (2010) showed that *miR172* molecules can move systemically from source to sink tissues in *Nicotiana benthamiana*. Earlier studies have shown that *miR172*, along with another miRNA (*miR156*), regulate phase transitions and flowering in Arabidopsis. *miR172* has been demonstrated to promote adult phase and flowering, whereas *miR156* is involved in juvenile stage development (Wu et al., 2009). Similar roles of *miR156* and *miR172* were also reported in rice (*Oryza sativa*; Xie et al., 2006) and maize (*Zea mays*; Chuck et al., 2007). Sequential action of both these miRNAs appears to be pivotal for phase transition and flowering in plant development. Flowering and tuberization are reproductive strategies that bear similar environmental cues and molecular players (Jackson, 2009). With the evidence of *miR172* being involved in both these pathways, we hypothesize that *miR156* could be involved in the potato tuberization pathway acting in concert with *miR172*.

miR156 is a well-conserved miRNA present in all land plants (Axtell and Bowman, 2008). It targets the transcripts of SQUAMOSA PROMOTER BINDING-LIKE (SPL) transcription factors and acts as a master regulator of plant development (Schwab et al., 2005). In Arabidopsis, *miR156* overexpression results in a prolonged juvenile phase and a delay in flowering, with increased branching and production of a large number of leaves (Huijser and Schmid, 2011). Similar phenotypes of *miR156* overexpression were also observed in rice (Xie et al., 2006), maize (Chuck et al., 2007), switchgrass (*Panicum virgatum*; Fu et al., 2012), and tomato (*Solanum lycopersicum*; Zhang et al., 2011b). In a recent study, Eviatar-Ribak et al. (2013) overexpressed the Arabidopsis *miR156* gene in potato (cv Desiree), where *miR156*-overexpressing lines exhibited suppressed leaf complexity and produced aerial tubers, indicating a role of *miR156* in tuberization. In addition to these functions, *miR156* and its targets, SPL transcription factors, have also been shown to regulate embryonic patterning (Nodine and Bartel, 2010), anthocyanin biosynthesis (Gou et al., 2011), and male fertility (Xing et al., 2010). Interestingly, *miR156* has also been detected in phloem sap of pumpkin (*Cucurbita maxima*; Yoo et al., 2004), Arabidopsis, apple (*Malus domestica*; Varkonyi-Gasic et al., 2010), and *Brassica napus* (Buhtz et al., 2008, 2010). miRNAs present in phloem exudates are proposed to be mobile, with a putative role as long-distance regulators of development and stress pathways by acting on target genes (Marín-González and Suárez-López, 2012). Although *miR156* is known to interact with the transcripts of SPL transcription factors, the mobility of *miR156* in plants has not yet been investigated.

In this study, we have identified and validated a *miR156a* precursor from potato. To understand the role of *miR156* and its target genes in potato development, we employed a number of strategies, including target gene validations, transgenic analysis, assays of *miR156* abundance, high-resolution mass spectrometry (HR-MS)-based hormone quantification, phloem sap analysis, and grafting. Our results suggest that *miR156* is a graft-transmissible signal that affects plant architecture and tuber development in potato. It is present in the phloem of wild-type plants, and it accumulates in short-day (SD)-induced stolons to facilitate tuber formation. In addition, *miR156* overexpression (OE) lines show multiple morphological changes and produce aerial tubers under inductive conditions. Although the formation of aerial tubers was recently demonstrated by Eviatar-Ribak et al. (2013), our study reveals additional novel functions of *miR156* in potato. Based on its accumulation in phloem sap of wild-type plants and its graft-transmissible effect, our results suggest that *miR156* moves through the phloem and regulates development in potato.

RESULTS

Identification, Validation, and Expression Analysis of *miR156* in Potato

miR156 was predicted to be present in potato by an in silico analysis reported earlier (Zhang et al., 2009). The MFold-predicted secondary structure (Zuker, 2003) of the *miR156a* precursor sequence (BI432985.1) had a hairpin loop with mature *miR156* in its stem region, a characteristic of miRNA precursors (Fig. 1A). To validate the presence of the *miR156a* precursor in potato, reverse transcription (RT)-PCR was performed, and the amplified fragment was sequence confirmed (Fig. 1B). A 20-bp mature *miR156* was detected by stem-loop end-point PCR in leaves and was verified by sequencing (Fig. 1C), demonstrating that *miR156* is expressed in potato.

The relative levels of *miR156* were analyzed by stem-loop quantitative reverse transcription (qRT)-PCR in potato plants of different age groups. Two-week-old plants showed higher accumulation of *miR156* in stem, and their levels decreased as the plant aged. However, *miR156* levels varied in mature leaves of plants of different ages (Fig. 1D). To determine whether *miR156* expression is regulated by the photoperiod, plants were grown under long-day (LD; tuber-noninductive) and SD (tuber-inductive) conditions. Stem-loop qRT-PCR analysis demonstrated a higher accumulation of *miR156* in leaves and stem under LD conditions as compared

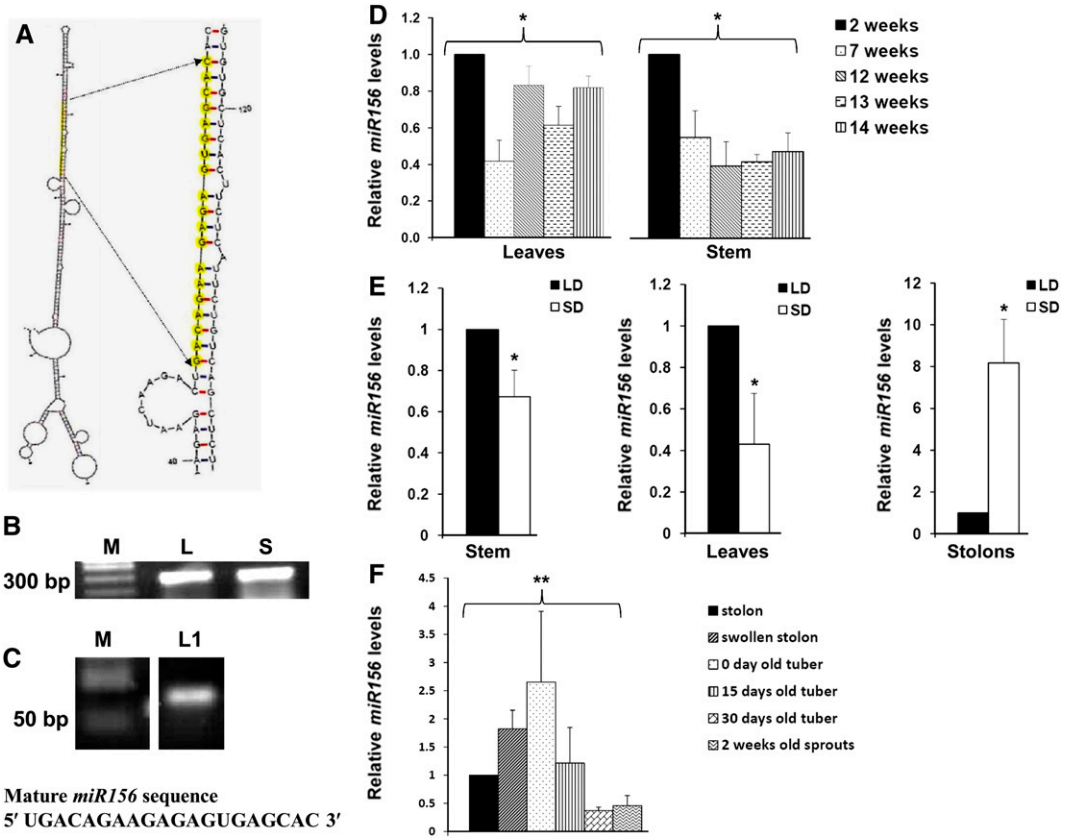

Figure 1. Identification, validation, and expression analysis of *miR156* in potato. A, Secondary structure of *miR156a* precursor as predicted by MFold (Zuker, 2003). Mature *miR156* sequence is highlighted in yellow. B, RT-PCR of *miR156a* precursor from leaf (L) and shoot (S). M represents a DNA marker. C, Stem-loop RT-PCR of mature *miR156* from leaves of LD-grown plants (L1). D, Age-specific *miR156* abundance in leaves and stem of wild-type potato grown under LD photoperiod. Error bars indicate SD of two biological replicates each with three technical replicates. Asterisks indicate one-factor ANOVA (*$P < 0.05$). E, *miR156* abundance in stem, leaves, and stolons of wild-type potato grown under LD and SD photoperiods for 15 dpi. Error bars indicate SD of three biological replicates each with three technical replicates. Asterisks indicate Student's *t* test (*$P < 0.05$). F, Relative abundance of *miR156* in different developmental stages of tuber formation and dormancy. Error bars indicate SD of three biological replicates each with three technical replicates. Asterisks indicate one-factor ANOVA (**$P < 0.01$). [See online article for color version of this figure.]

with the plants under the SD photoperiod (Fig. 1E). However, in stolons, *miR156* levels were found to be approximately 8-fold higher under SD as compared with LD photoperiod (Fig. 1E). Our analysis showed a range of *miR156* abundance in swollen stolons, tubers stored postharvest for different time periods (0, 15, and 30 d), and 2-week-old sprouts. Zero-day-old tubers (postharvest) showed an approximately 2.5-fold higher accumulation than in stolons harvested from SD-induced plants, whereas *miR156* levels in juvenile tuber sprouts were almost half the level in stolons (Fig. 1F). Overall, our expression analysis suggests that *miR156* shows tissue-specific accumulation with respect to the age of the plant and the photoperiod.

Overexpression of *miR156* Affects Multiple Morphological Traits

The level of *miR156* in *miR156* OE lines (*miR156* OE 5.1 and 6.2) was determined by stem-loop qRT-PCR (Supplemental Fig. S1, A and B). Two-week-old OE lines exhibited a drastic change in leaf phenotype (Fig. 2, A and B), and as they matured, they did not form an inflorescence compared with wild-type plants (Fig. 2, C and D). These plants did not flower even after 18 weeks of growth, whereas wild-type plants produced inflorescences in 12 weeks. *miR156* OE plants also exhibited enhanced branching from axillary buds and an increased number of nodes, resulting in a bushy appearance (Fig. 2, E–H). The fresh weight of roots in OE lines was also significantly reduced (Fig. 2I). The leaf architecture of *miR156* OE lines was dramatically affected. *miR156* OE plants produced smaller leaves with reduced leaflet number (Fig. 3, A and B). The venation pattern was found to be altered such that the side veins of transgenic leaves were less prominent (Fig. 3, C and D). Transverse sections of leaves showed disoriented cell arrangement as well as the presence of large epidermal cells in the *miR156* OE 5.1 line (Fig. 3, E and F). We also observed a reduction in stomatal

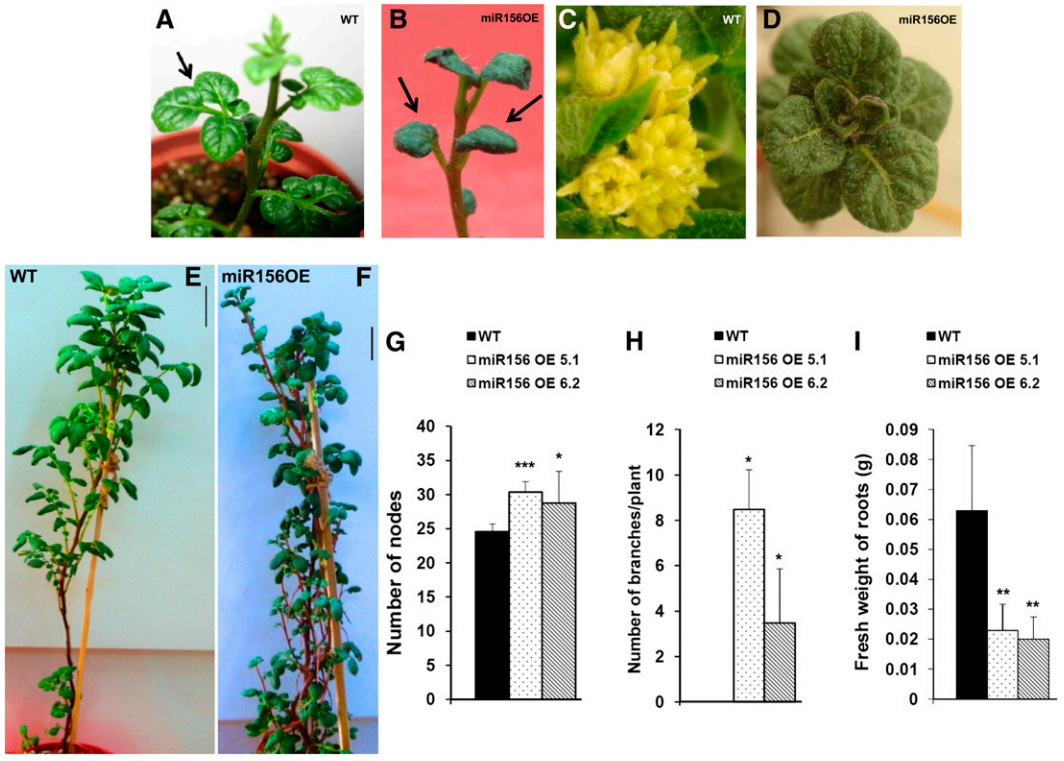

Figure 2. Overexpression of *miR156* affects multiple morphological traits in potato. A and B, Two-week-old plants of the wild type (WT; A) and *miR156* OE 5.1 (B). C and D, Inflorescence produced at the apical tip of 12-week-old wild-type potato plants (C), while *miR156* OE 5.1 plants of the same age produced leaves (D). E and F, Twelve-week-old plants of wild-type (E) and *miR156* OE 5.1 (F) lines of potato. Bars = 5 cm. G to I, Number of nodes (G; $n = 5$), number of axillary branches (H; $n = 4$), and fresh weight of roots (I; $n = 6$) of wild-type and *miR156* OE plants. Error bars indicate SD. Asterisks indicate statistical differences as determined using Student's *t* test (***$P < 0.001$, **$P < 0.01$, *$P < 0.05$). [See online article for color version of this figure.]

density in both OE lines as opposed to the wild type (Fig. 3, G–J). In addition, trichome number was reduced with an increase in trichome length in OE lines (Fig. 3, K–O). To gain more insight into the function of *miR156*, 35S::*miR156* tobacco (*Nicotiana tabacum*) plants were generated. All the tobacco OE plants showed a similar phenotype to that observed in *miR156* OE potato plants (Supplemental Fig. S2).

miR156 Regulates Potato Tuberization

To examine whether an increase in *miR156* levels in OE lines could have any impact on tuber development, we examined the tuberization phenotype of the *miR156* OE 5.1 and 6.2 lines. OE line 5.1 produced aerial and underground tubers after 4 weeks of SD induction, whereas wild-type plants grown under an SD photoperiod only produced underground tubers (Fig. 4, A–C). Line 6.2 produced underground tubers and showed a delayed formation of aerial tubers. None of the plants produced tubers under the LD photoperiod.

Overall, *miR156* OE lines (5.1 and 6.2) developed fewer underground tubers and showed reduced tuber yields (Table I). Previous reports have shown *miR172* and the *Flowering Locus T*-like paralog *StSP6A* to act as positive regulators of tuberization (Martin et al., 2009; Navarro et al., 2011). Since *miR156* OE lines exhibited reduced tuber yield, we investigated the levels of *StSP6A* and *miR172* (tuberization markers) in leaves of OE plants. Also, *miR172* levels were quantified in SD-induced stolons. Our results showed a reduction in the levels of the tuberization markers *miR172* and *StSP6A* in *miR156* OE lines. *miR172* levels were reduced by approximately 80% in leaves and stolons, while *StSP6A* levels were reduced by approximately 60% in leaves (Fig. 4, D–F).

Zeatin Riboside and Orobanchyl Acetate Levels Are Affected by *miR156* Overexpression

miR156 overexpression in potato resulted in a drastic phenotype of increased branching, a higher number of leaves with reduced leaflets, and a delay in flowering, a phenotype that was also recently described for tomato LONELY GUY1 (TLOG1) overexpression in tomato (Eviatar-Ribak et al., 2013). LONELY GUY1 (LOG1) is a cytokinin biosynthetic gene that converts cytokinin ribosides to biologically active cytokinin (Kurakawa et al., 2007). Considering the role of cytokinins in branching (Domagalska and Leyser, 2011), we investigated the effect of *miR156* on the cytokinin pathway. *miR156* OE plants

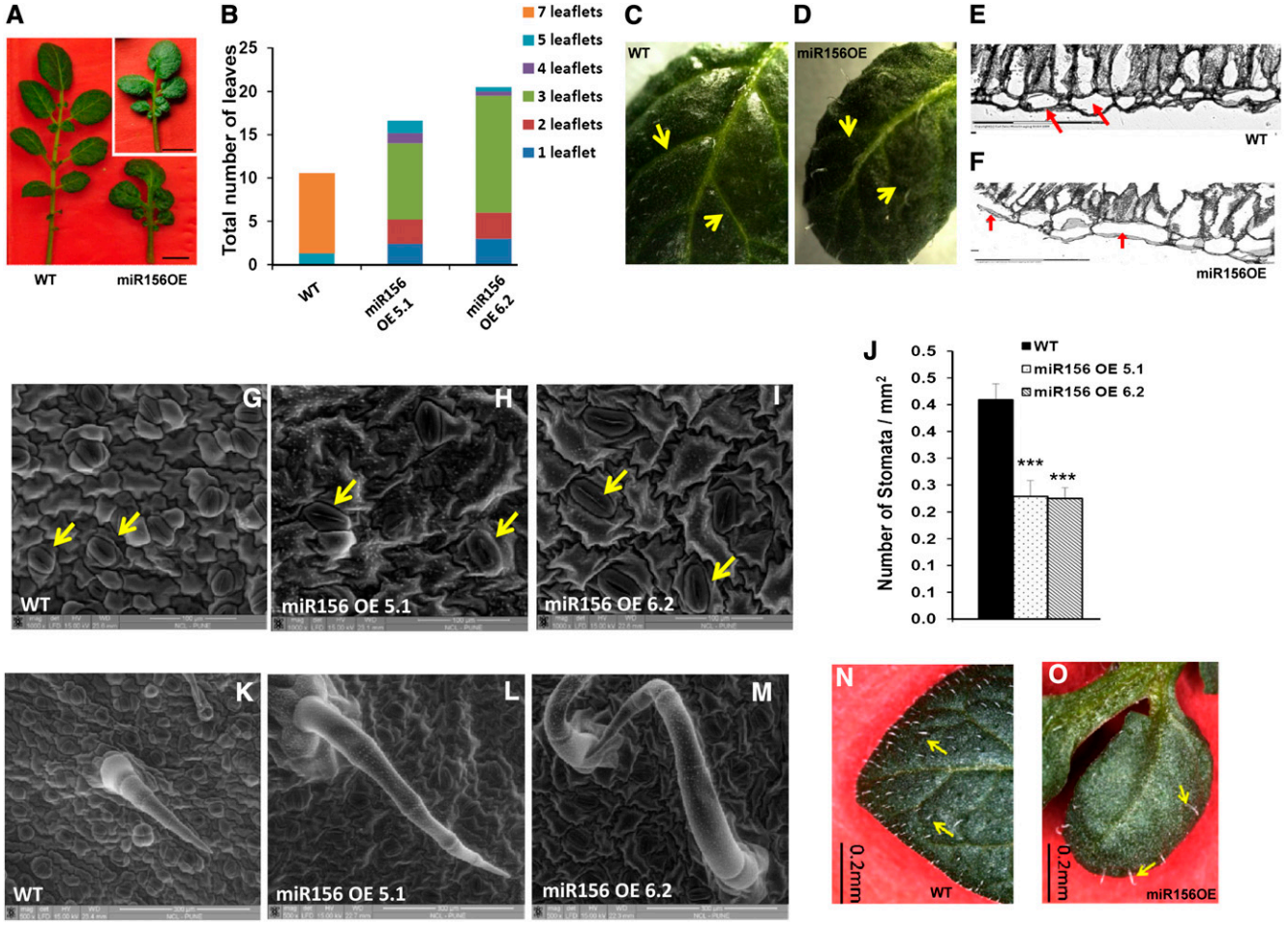

Figure 3. Effect of *miR156* overexpression on leaf development of potato. A, Leaves of 8-week-old wild-type (WT) and *miR156* OE 5.1 and 6.2 (inset) plants. Bars = 1 cm. B, Distribution of the number of leaflets per leaf in 8-week-old wild-type and *miR156* OE 5.1 and 6.2 plants. C and D, Venation pattern of wild-type leaf (C) and *miR156* OE 5.1 leaf (D). Arrows indicate veins. E and F, Transverse sections of leaves (20×) of wild-type (E) and *miR156* OE 5.1 (F) plants showing differences in leaf architecture. The epidermal cells are marked by arrows. G to I, eSEM images of the leaf surface showing differences in the size of epidermal cells and stomata (marked by arrows) for wild-type (G) and *miR156* OE 5.1 (H) and *miR156* OE 6.2 (I) plants. Bars = 100 μm. J, Stomatal density of wild-type and *miR156* OE 5.1 and 6.2 plants ($n = 5$). Error bars indicate SD. Asterisks indicate statistical differences as determined using Student's *t* test (***$P < 0.001$). K to M, eSEM images of trichomes for wild-type (K) and *miR156* OE 5.1 (L) and *miR156* OE 6.2 (M) plants. Bars = 300 μm. N and O, Trichome phenotype of wild-type leaf (N) and *miR156* OE 5.1 leaf (O). Bars = 0.2 mm. [See online article for color version of this figure.]

showed approximately 1.8-fold increased expression of *StLOG1* in the axillary meristems as compared with wild-type plants (Fig. 5A). Also, the levels of *StCyclin D3.1*, a cytokinin-responsive gene, were increased up to approximately 8-fold as compared with wild-type plants (Fig. 5B). To determine the amount of cytokinin (zeatin riboside), HR-MS analysis demonstrated increased levels (more than 2-fold) in *miR156* OE plants as compared with the wild type in both SD and LD conditions (Fig. 5C; Supplemental Figs. S3 and S4). As strigolactones are also considered to be branching hormones (Domagalska and Leyser, 2011), we investigated the levels of one such strigolactone: orobanchyl acetate. HR-MS analysis demonstrated reduced levels of orobanchyl acetate (approximately 20% under LD conditions and approximately 60% under SD conditions) in *miR156* OE plants as compared with the wild type (Fig. 5D; Supplemental Figs. S5 and S6). The changes in these hormone amounts correlated with the branching phenotype observed in *miR156* OE lines.

miR156 Targets *StSPL* Transcription Factors

Our in silico analysis with psRNATarget software (plantgrn.noble.org/psRNATarget; Dai and Zhao, 2011) predicted 12 potential target genes for *miR156* in potato (Supplemental Table S1). Further analysis of these target genes revealed that nine out of the 12 genes (including LIGULELESS1 [LG1]) belong to the SPL family of transcription factors. Two belong to the DNA topoisomerase family of proteins, while one target is of unknown function. Additionally, we have

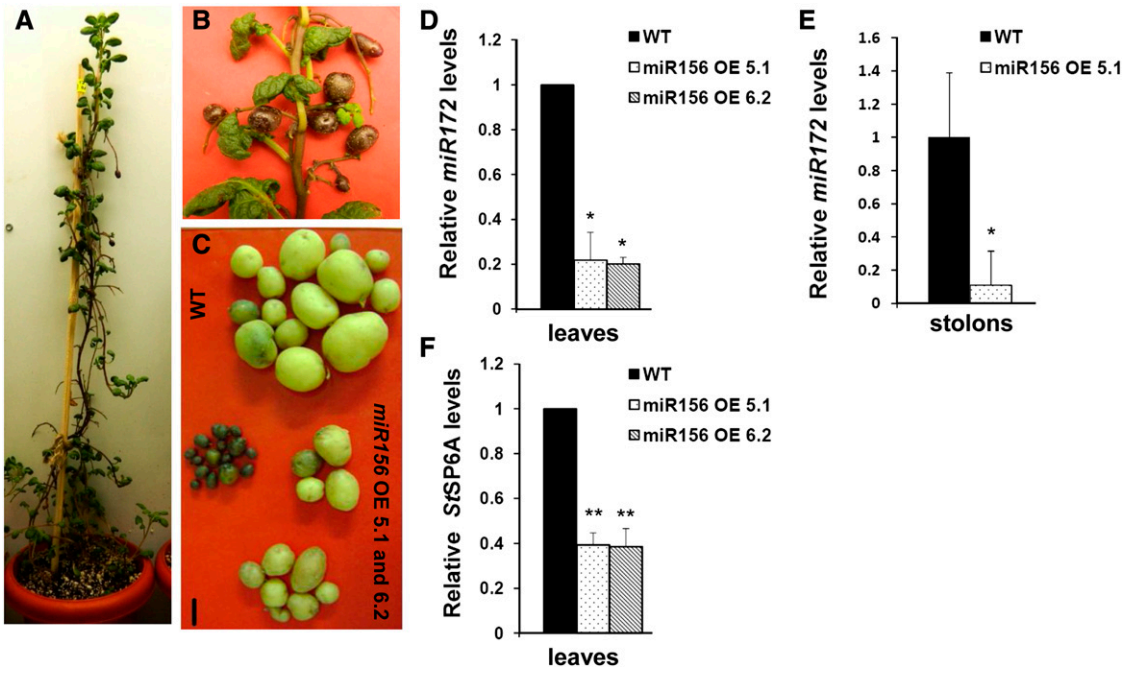

Figure 4. *miR156* regulates potato tuberization. A, *miR156* OE 5.1 plant incubated for 30 d under SD conditions. B, Aerial tubers developed on *miR156* OE 5.1. C, Tubers of representative wild-type (WT) and miR156 OE line 5.1 and 6.2 plants. Bar = 1 cm. D to F, Levels of tuberization markers: miR172 in 8-d post SD-induced leaves of wild-type and miR156 OE line 5.1 and 6.2 plants (D); *miR172* in 15-d post SD-induced stolons of wild-type and *miR156* OE line 5.1 plants (E); and *StSP6A* in 8-d post SD-induced leaves of wild-type and *miR156* OE line 5.1 and 6.2 plants (F). For *miR172* in leaves (D), error bars indicate SD of two biological replicates each with three technical replicates; for *miR172* in stolons (E; 15 dpi in SD conditions), error bars indicate SD of one biological replicate with three technical replicates; for *StSP6A* (F), semiquantitative analysis was performed with three independent replicates. Error bars indicate SD of three replicates. Asterisks indicate statistical differences as determined using Student's *t* test (*$P < 0.05$, **$P < 0.01$). [See online article for color version of this figure.]

also predicted all these target genes by TargetAlign software. Finally, based on their scores and consistency of analysis in both softwares, we short listed five *miR156* target genes, *StSPL3*, *StSPL6*, *StSPL9*, *StSPL13*, and *StLG1*, for further analysis. To determine if these genes are the targets of *miR156* in potato, modified RNA ligase-mediated (RLM) 5′ RACE was performed. RNA sequences with 5′ termini corresponding to the 10th/11th nucleotides of *miR156* were consistently detected, demonstrating that *StSPL6*, *StSPL9*, *StSPL13*, and *StLG1* are targeted by *miR156* in vivo (Fig. 6, A and B). However, *StSPL3* was cleaved at sites other than the 10th/11th nucleotides of *miR156*, which is not a common observation in plant miRNAs. Levels of these targets were also quantified in *miR156* OE plants. As expected, transcript levels of these targets showed different degrees of reduction (*StSPL3*, approximately 80%; *StLG1*, 70%; *StSPL13*, 60%; *StSPL9*, 40%; and *StSPL6*, 30% in *miR156* OE 5.1 plants [Fig. 6C]). Our results are consistent with previous studies on the *miR156*-SPL interaction (Schwab et al., 2005).

Regulation of *miR172* by the *miR156*-SPL Module

Overexpression of *miR156* in potato resulted in lower tuber yields and reduced levels of *miR172* and *SPLs* as mentioned above. Our bioinformatic analysis of the StMIR172b promoter showed the presence of multiple GTAC motifs, characteristic of SPL binding (Birkenbihl et al., 2005). We chose to continue our investigation with StSPL9, since the *miR156*-SPL9 interaction has previously been demonstrated in Arabidopsis (Wu et al., 2009) and rice (Jiao et al., 2010), suggesting that a similar interaction module might also be conserved in potato. To examine if StSPL9 binds to the StMIR172b promoter, gel retardation assays were performed. The StMIR172b promoter was analyzed in four fragments (P1–P4; Fig. 7A), having two binding motifs in the P1 fragment, a single motif each in P2 and P3, while P4 served as a negative control. Recombinant StSPL9 protein (42 kD) retarded the mobility of the P1 promoter sequence, whereas the other three promoter

Table I. *Tuber yields (tuber number and weight) of wild-type and miR156 OE 5.1 and 6.2 plants incubated under SD conditions for 30 d*

Means of three plants each were calculated.

Plant	No. of Tubers	Weight of Tubers
		g
Wild type	13.0 ± 1.73	37.7 ± 2.75
miR156 OE 5.1	4.66 ± 1.15	5.83 ± 0.75
miR156 OE 6.2	7 ± 1.0	6.52 ± 2.55

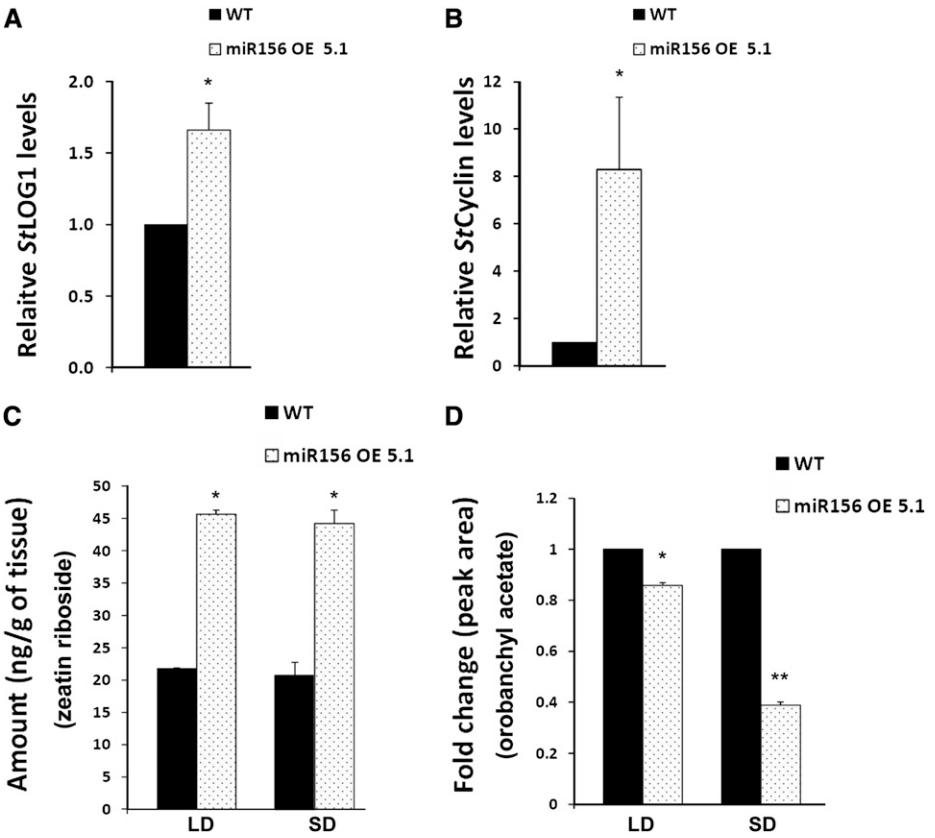

Figure 5. Zeatin riboside and orobanchyl acetate levels are affected by *miR156* overexpression. A and B, qRT-PCR analysis of *StLOG1* (A) and *StCyclin D3.1* (B) in axillary meristems of wild-type (WT) and miR156 OE 5.1 plants incubated for 15 d under SD conditions. Error bars indicate SD of three biological replicates each with three technical replicates. Asterisks indicate statistical differences as determined using Student's *t* test (*$P < 0.05$). C and D, HR-MS analysis of wild-type and *miR156* OE 5.1 plants for zeatin riboside (C) and orobanchyl acetate (D). The tissues were axillary meristems of wild-type and *miR156* OE 5.1 plants incubated for 15 d under both SD and LD conditions. Error bars indicate SD of two biological replicates. Asterisks indicate statistical differences as determined using Student's *t* test (*$P < 0.05$, **$P < 0.01$).

fragments (P2–P4) remained unaffected (Fig. 7B). Competition gel retardation assays were performed with ^{32}P-labeled and unlabeled P1 fragment. With increased unlabeled P1, the P1-SPL9 complex was diminished over time (Fig. 7C). Our analysis demonstrated StSPL9-MIR172 promoter interactions in vitro, with StSPL9 binding to a promoter region with two binding sites.

To further validate the *miR156*-StSPL9 interaction, we generated *miR156*-resistant StSPL9 OE potato plants (rSPL9 OE lines) driven by the cauliflower mosaic virus (CaMV) 35S promoter (Supplemental Fig. S7, A and B). rSPL9 transgenics were generated by introducing silent mutations in the microRNA recognition element (MRE), so that the mutated transcript is no longer recognized by *miR156*. Stem-loop qRT-PCR analysis revealed an approximately 5-fold increase in levels of *miR172* under SD conditions compared with the wild type (Fig. 7D). This increase in *miR172* levels under SD conditions, however, was not reflected by the tuberization phenotype of the rSPL9 OE line (Supplemental Fig. S7C).

Detection of *miR156* in Phloem of Wild-Type Potato

In order to investigate the presence of *miR156* in phloem of potato plants, we harvested phloem cells by laser microdissection pressure catapulting (LMPC) and tested for the presence of *miR156* in phloem cells of wild-type potato (Fig. 8, A and B). While *miR156* was detected in phloem cells, we did not detect the *miR156*a precursor in phloem sap harvested from wild-type plants (Fig. 8C). The purity of phloem sap (phloem-enriched exudate) was confirmed by detecting the phloem-specific transcript G2-like transcription factor and the absence of root-specific transcript nitrate transporter (Fig. 8D). The *miR156** strand, however, was detected in phloem sap exudates of wild-type plants by stem-loop qRT-PCR (Fig. 8E). To understand if photoperiod has any role in *miR156* accumulation in the phloem, we also carried out a stem-loop qRT-PCR analysis of phloem sap harvested from wild-type plants incubated for 8, 15, and 30 d post induction (dpi) under both SD and LD conditions. Higher accumulation of *miR156* was observed in phloem sap harvested from 8- and 15-dpi SD-induced plants, indicating that *miR156* accumulation increased under SD conditions in phloem sap of potato. This pattern changed in plants incubated for longer times (30 dpi; Fig. 8F).

miR156 Is Potentially a Graft-Transmissible Signal in Potato

In our study, we detected *miR156* in LMPC-harvested phloem cells, and it exhibited an SD-induced accumulation

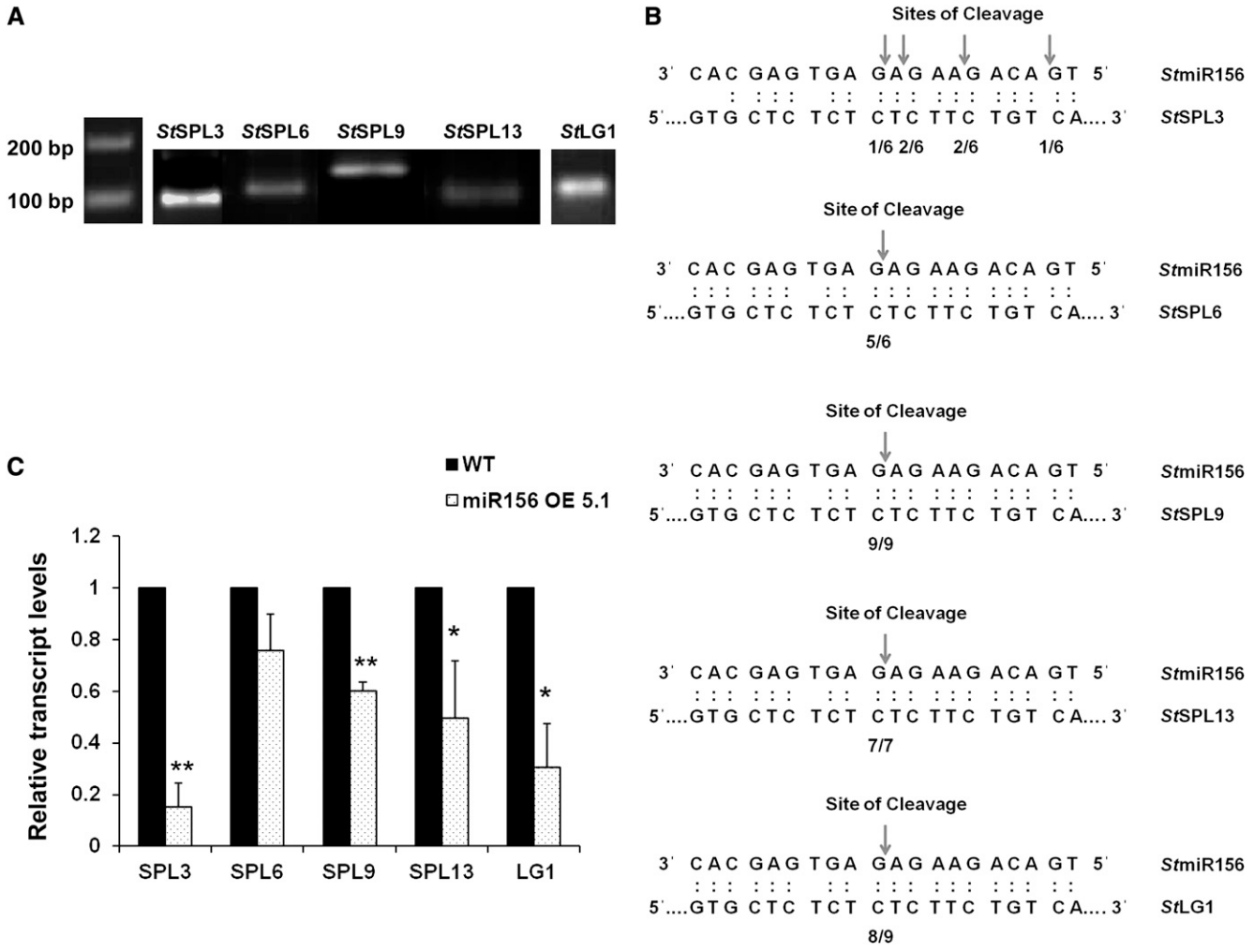

Figure 6. *miR156* targets in potato. A and B, *miR156* cleavage site mapping in *miR156* targets as determined by modified RLM-RACE. A, Nested PCR products were cloned and sequenced. B, Frequency of 5′ RACE clones showing cleavage site (arrows) and fractions indicating proportions of clones showing these cleavage sites. C, Expression pattern of *StSPL3*, *StSPL6*, *StSPL9*, *StSPL13*, and *StLG1* in wild-type (WT) and *miR156* OE 5.1 plants by qRT-PCR. Error bars indicate SD of three biological replicates each with three technical replicates. Asterisks indicate statistical differences as determined using Student's *t* test (*$P < 0.05$, **$P < 0.01$).

pattern in phloem sap. Considering this observation, we tested whether *miR156* is a phloem-mobile signal in potato. Grafting experiments (homografts, heterografts, and reverse grafts) were performed to demonstrate the mobility of *miR156* (Fig. 9A). After 4 weeks of SD induction, analysis of morphological changes in grafts as well as the quantitative analysis of *miR156* were performed. Overall, the leaf shape and trichome morphology of stocks from the heterografts (*miR156* OE plants as scion and the wild type as stock) were affected. The newly emerging leaves from the axillary shoots on the stock of heterografts had more prominent but fewer trichomes (Fig. 9B) and exhibited small and thick lamina along with reduced numbers of leaflets (Fig. 9C). On the other hand, newly emerging leaves from wild-type scions of reverse grafts did not show any phenotype similar to *miR156* OE plants (Fig. 9D). All the heterografts had less tuber yield as compared with homografts, while reverse grafts did not form any tubers (Table II).

The morphological changes in the stock stems of heterografts could be due to (1) the transport of mature *miR156* itself, (2) the transport of the overexpressed *miR156a* precursor transgene, or (3) a *miR156*-mediated up-regulated mobile factor activating *miR156* transcription in stock stems. To analyze if mature *miR156* is transported, we carried out a quantitative analysis by stem-loop qRT-PCR. In stock stems of all four heterografts, a higher accumulation of mature *miR156* was observed, as opposed to homografts (Fig. 9E). On the other hand, absence of the *miR156a* precursor transgene in heterograft stock stems confirmed that the overexpressed transgene is not moving from scion to stock (Fig. 9F). Also, a comparative analysis of mature *miR156*

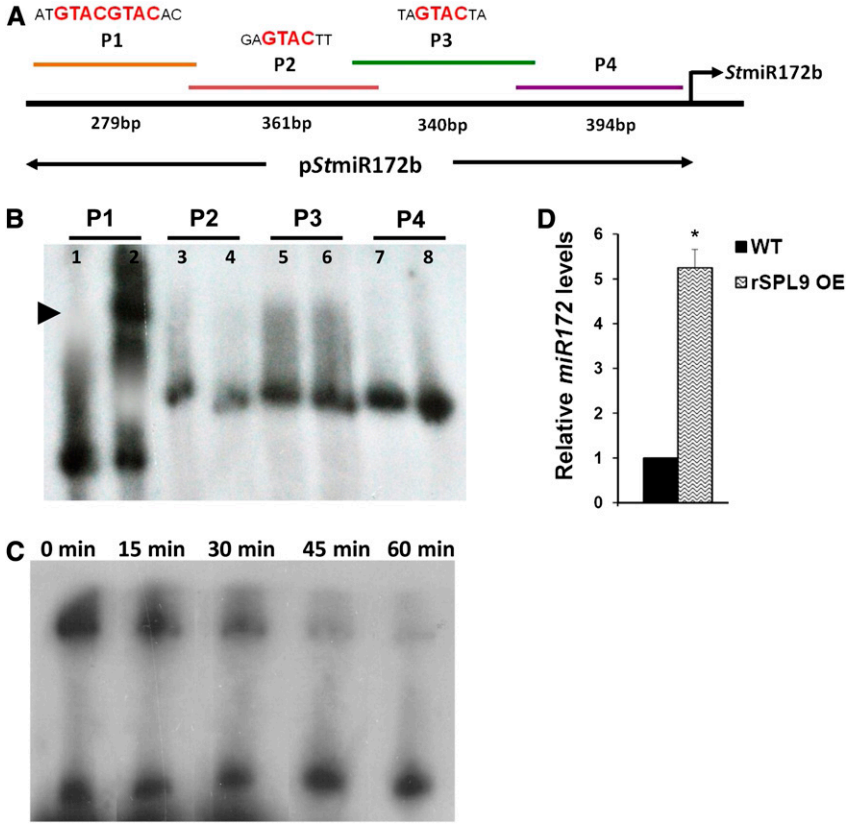

Figure 7. StSPL9 binds to the StMIR172b promoter. A, Schematic representation of StMIR172b promoter sequence showing SPL binding motifs and lengths of four fragments. B, Gel retardation assay of StMIR172b promoter fragments P1 to P4 with StSPL9. The lanes are alternate for free probe and probe + protein. C, Cold competition retardation assay of P1 with StSPL9. Labeled P1 was incubated with StSPL9 for 30 min at 25°C, and then a 100-fold molar excess of unlabeled P1 was added and aliquots were analyzed after the indicated times (0–60 min). D, Relative levels of *miR172* in 15-d post SD-induced leaves of wild-type (WT) and rSPL9 OE plants. Error bars indicate SD of two biological replicates each with three technical replicates. The asterisk indicates a statistical difference as determined using Student's *t* test ($*P < 0.05$). [See online article for color version of this figure.]

and *miR156a* precursor levels in both wild-type and grafted plants clearly demonstrated that mature *miR156* had a higher accumulation than its precursor form (Supplemental Fig. S8, A–D). These findings make the possibility of *miR156a* precursor transgene movement as well as activated localized transcription of *miR156* in stock stems of heterografts unlikely. Instead, the higher accumulation of mature *miR156* in heterograft stock stems supports the preferential transport of mature *miR156* itself, from scion to stock in grafted plants. Overall, our results suggest that *miR156* is a graft-transmissible phloem-mobile signal that affects tuberization and plant architecture in potato.

DISCUSSION

miR156 in Potato

Several reports have previously demonstrated the function of *miR156* in various plant species like maize (Chuck et al., 2007), Arabidopsis (Huijser and Schmid, 2011), switchgrass (Fu et al., 2012), rice (Xie et al., 2006), tomato (Zhang et al., 2011b), and poplar hybrid (*Populus trichocarpa*; Wang et al., 2011). Earlier studies (Zhang et al., 2009; Yang et al., 2010; Xie et al., 2011) have predicted *miR156* in potato through a bioinformatic approach. The recent study by the Tomato Genome Consortium (2012) reported 13 members of the miR156 family in potato, whereas the miR156 family has 12 members in Arabidopsis, 12 in rice, and 11 in poplar hybrid (Griffiths-Jones et al., 2008). A very recent report (Eviatar-Ribak et al., 2013) has shown that overexpression of *miR156* in the potato cv Desiree (a day-neutral cultivar) resulted in stolon-borne aerial mini tubers from almost all of the distal buds. *miR156* OE plants had exhibited late flowering, suppression of leaf complexity, and a profuse branching phenotype. We had similar observations for *miR156* overexpression in potato, but in the photoperiod-sensitive subspecies *andigena* 7540. We wanted to investigate the following. (1) Does *miR156* affect multiple morphological traits other than what was already observed in potato? (2) What could be the target genes of *miR156* and their roles in potato? (3) What is the role of *miR156* in tuberization under different photoperiods? (4) Knowing its presence in phloem of other plant species, our hypothesis was to test if *miR156* acts as a potential mobile signal in potato development.

To answer these questions, we started with validating the presence of one member of the *miR156* family, *miR156a* in potato. This is different from the approach followed in a previous report (Eviatar-Ribak et al., 2013), where the Arabidopsis *miR156a* precursor was overexpressed in potato. The sequence of mature potato *miR156* was found to be identical to that of *miR156* of Arabidopsis, rice, maize, and sorghum (*Sorghum bicolor*), suggesting its conserved nature. In our analysis,

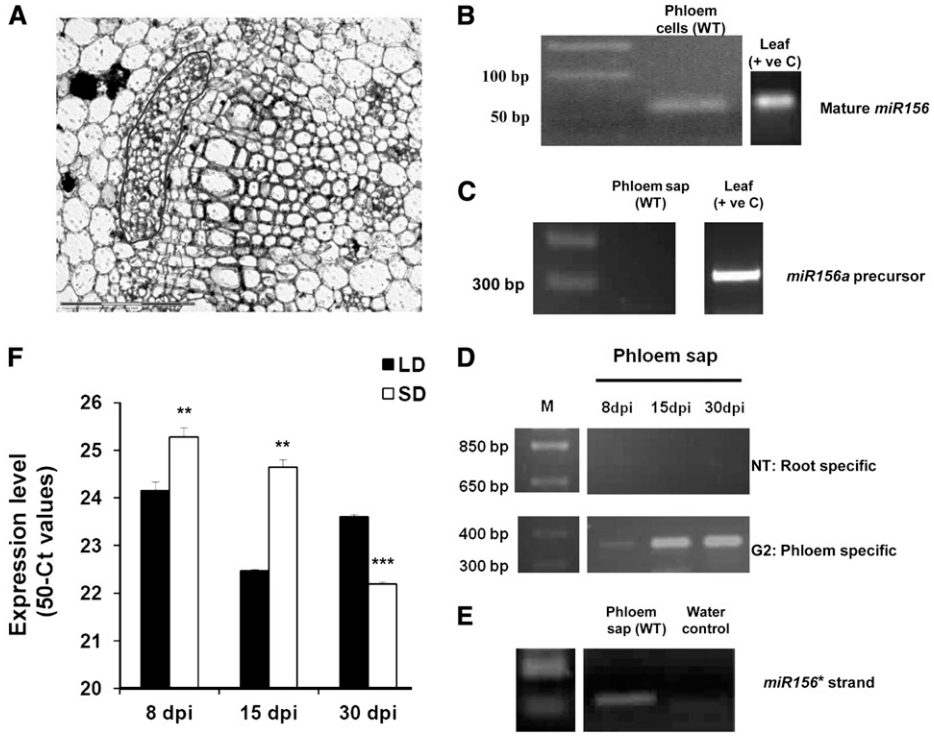

Figure 8. Detection of *miR156* in phloem. A, Phloem tissue in a wild-type stem section (marked in red). This tissue was harvested by LMPC. B, Detection of *miR156* (mature) in phloem of wild-type plants (WT) and leaf tissue of wild-type plants (positive control [+ ve C]) by stem-loop RT-PCR. C, Absence of *miR156a* precursor (300 bp) in wild-type phloem sap and its presence in wild-type leaf, acting as a positive control, by RT-PCR analysis. D, RT-PCR analysis of nitrate transporter (NT; root-specific transcript) and G2-like transcription factor (G2; phloem-specific transcript) of potato phloem sap of the wild type (phloem-enriched exudate) to assess its purity (Banerjee et al., 2006a). E, Detection of the *miR156** strand in phloem sap of the wild type by stem-loop RT-PCR. F, Differential accumulation of *miR156* (mature) under SD and LD photoperiods in phloem sap of wild-type plants harvested after 8, 15, and 30 dpi. *miR156* accumulation is plotted as 50 minus Ct (for cycle threshold; 50-Ct) values as described previously (Pant et al., 2008). Error bars indicate SD of one biological replicate with three technical replicates. Asterisks indicate statistical differences as determined using Student's *t* test (**$P < 0.01$, ***$P < 0.001$).

miR156 exhibited an age-dependent expression pattern in potato stem tissues, and its levels decreased as the plant aged (Fig. 1D). This observation was consistent with the earlier studies in Arabidopsis and rice (Wu et al., 2009; Xie et al., 2012). Both of these reports showed a gradual decrease of the expression of *miR156* in shoots as the plant aged. However, in developing leaves of rice, an opposite expression pattern of *miR156* was demonstrated. In our study, no significant pattern of *miR156* expression was observed in leaves (Fig. 1D). All of the previous reports mentioned above demonstrate decreased *miR156* expression with respect to plant age, suggesting its role in juvenile phase maintenance. However, photoperiod-mediated expression and function of *miR156* have not been documented earlier. Because tuberization in potato is a photoperiod-regulated process, we investigated the effect of the photoperiod on *miR156* expression and its function. Our analysis suggests that *miR156* is differentially expressed under SD/LD conditions in a tissue-specific manner (Fig. 1, E and F). As we have validated the *miR156a* precursor in potato, we carried out bioinformatic analysis of the upstream sequence of the MIR156a gene using the PLACE online tool (Higo et al., 1999). The MIR156a upstream sequence exhibited a number of light regulatory motifs (Supplemental Table S2; Waksman et al., 1987; Vorst et al., 1990; Vauterin et al., 1999), indicating a putative light-mediated regulation of this miRNA along with an endogenous, age-mediated regulation.

Overexpression of *miR156* Affects Plant Architecture in Potato and Tobacco

In our study, *miR156* OE lines (potato and tobacco) exhibited phenotypes like profuse axillary branching, altered leaf and trichome morphology, and delayed or no flowering, documented earlier in a number of plants such as Arabidopsis (Huijser and Schmid, 2011), rice (Xie et al., 2006), tomato (Zhang et al., 2011b), and potato (Eviatar-Ribak et al., 2013). In addition to these phenotypes, an altered venation pattern in leaves, disoriented cell organization with larger epidermal

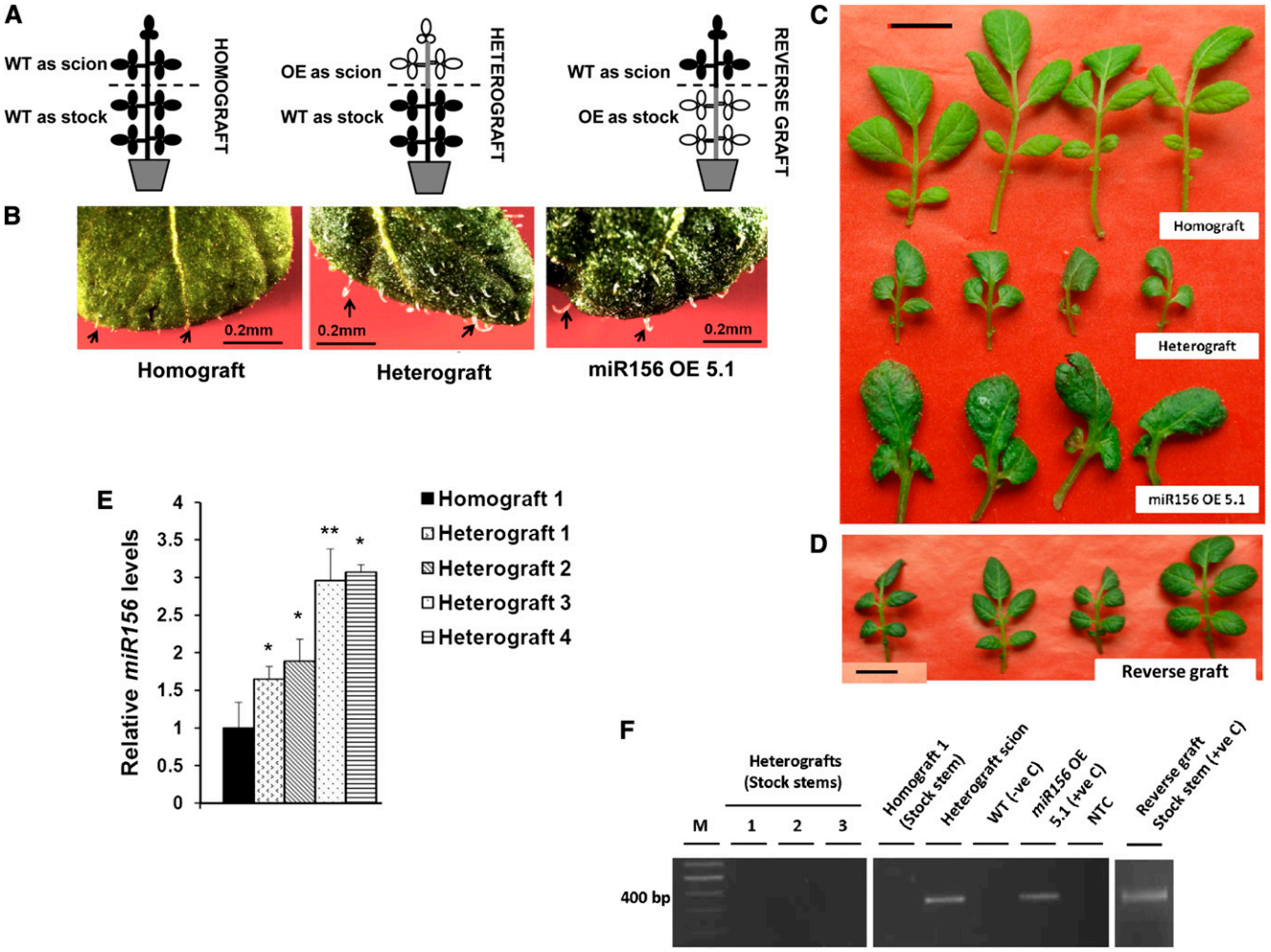

Figure 9. *miR156* is a potential graft-transmissible signal. A, Pictorial representation of the grafts. WT, Wild type. B, Trichomes of homograft (stock leaves), heterograft (stock leaves), and leaves from *miR156* OE 5.1 plants, where trichomes in heterografts (stock leaves) are less in number and more in length, as observed for *miR156* OE 5.1 plants. Bars = 0.2 mm. C and D, Leaves of homograft (stock), heterograft (stock), *miR156* OE 5.1 plants, and reverse grafts (scion), where heterograft stock leaves mimic the phenotype of *miR156* OE 5.1 leaves (C), while reverse graft scion leaves mimic the phenotype of homograft leaves (stock; D) Bars = 1 cm. E, Relative levels of mature *miR156* in stock stems of four representative heterografts (1–4) and homograft incubated under SD conditions and harvested after 30 dpi were measured by stem-loop qRT-PCR. Error bars indicate SD of one biological replicate with three technical replicates. Asterisks indicate statistical differences as determined using Student's *t* test ($*P < 0.05$, $**P < 0.01$). F, Detection of *miR156a* precursor transgene in stock stems of homograft, three representative heterografts (1–3), and reverse graft by RT-PCR analysis. Stem tissue of heterograft scion, reverse graft stock, and a *miR156* OE 5.1 plant served as positive controls (+ve C), with the wild type as a negative control (−ve C). NTC, No template control. [See online article for color version of this figure.]

cells, and reduced stomatal density and root biomass were also observed in both the OE lines (Figs. 2 and 3), indicating several new functions for *miR156* in potato. Overall, this suggests that *miR156* acts as a master regulator involved in the regulation of different plant developmental traits. The altered leaf morphology in OE plants can possibly be a result of reduced levels of *SPLs* (Fig. 6C). A number of previous reports (Wu and Poethig, 2006; Shikata et al., 2009; Usami et al., 2009; Chen et al., 2010) have described the role of SPLs in leaf development in Arabidopsis, suggesting that *StSPLs* might control leaf size and shape, altered venation, and reduced leaflet number in potato as well. LG1 is a well-characterized SPL protein whose function in leaf development has previously been reported in maize (Harper and Freeling, 1996) and rice (Lee et al., 2007). It was shown to be involved in controlling ligule and auricle development and the formation of a laminar joint between leaf blade and leaf sheath. In our study, reduced *StLG1* expression in *miR156* OE plants could possibly explain the aberrant leaf morphology (reduced leaf lamina and curled leaf margins). To understand the cause of the profuse branching phenotype of *miR156* OE plants in potato, we quantified the amounts

Table II. *Number of tubers of homografts, heterografts, and reverse grafts incubated under SD conditions for 30 d*

Means of three grafted plants were calculated.

Graft	No. of Tubers
Homografts	9.5 ± 2.12
Heterografts	2 ± 1.41
Reverse grafts	0 ± 0

of cytokinin and strigolactone, hormones that are known to play an important role in branching (Domagalska and Leyser, 2011). Cytokinins act antagonistically to auxins and promote branching from axillary meristems, leading to the loss of apical dominance (Domagalska and Leyser, 2011). *miR156* OE plants exhibited increased levels (more than 2-fold) of zeatin riboside under both SD and LD photoperiods (Fig. 5C), which is consistent with the bushy phenotype of these OE plants. Increased cytokinin amount was also accompanied by increased expression of the cytokinin biosynthesis gene *StLOG1* and the cytokinin-responsive gene *StCyclin D3.1* (Fig. 5, A and B). This increase in the activity of cytokinin might have caused the profuse branching phenotype. On the other hand, in Arabidopsis, strigolactone mutants show increased branching (Gomez-Roldan et al., 2008). In our study as well, *miR156* OE plants contained reduced amounts of orobanchyl acetate (Fig. 5D). The absence of flowering in both potato and tobacco OE plants supports the role of *miR156* in controlling phase transitions. In Arabidopsis, AtSPL2, AtSPL3, AtSPL9, AtSPL10, and AtSPL11 are shown to act as positive regulators in promoting floral meristem identity by directly regulating genes like LEAFY, FRUITFUL, and APETALA1 (Chen et al., 2010). A similar mechanism might also be conserved in potato, since *StSPL3* and *StSPL9* are found to be reduced in *miR156* OE plants (Fig. 6C).

miR156 Regulates Potato Tuberization

Flowering and tuberization are different reproductive strategies, both of which are photoperiod-mediated mechanisms (Jackson, 2009). Several molecular components like phytochrome B (Jackson et al., 1998), CONSTANS (Martinez-Garcia et al., 2002), and StSP6A (Navarro et al., 2011) have previously been shown to play roles in flowering and potato tuberization. In addition, two other miRNAs (*miR156* and *miR172*) were shown to control developmental timing and flowering in Arabidopsis (Wu et al., 2009). The positive role of *miR172* in tuberization was reported earlier (Martin et al., 2009), while a very recent report (Eviatar-Ribak et al., 2013) demonstrated the role of *miR156* in tuber formation. In Arabidopsis, *miR156* regulates *miR172* expression via AtSPL9 (Wu et al., 2009) during phase transitions. Similarly, we observed reductions of *miR172* and *StSPL9* in *miR156* OE lines (Figs. 4, D and E, and 6C) in potato. Although in our analysis, *StSPL9* was found to be reduced by 40%, there is a possibility of *miR156* acting on StSPL9 by translational arrest as well (Gandikota et al., 2007). Gel retardations assays confirmed the regulatory role of the *miR156*-SPL-*miR172* module in potato. However, control of *miR172* by SPLs other than StSPL9 cannot be ruled out. This regulatory module is likely to be active in leaves induced under LD conditions, as there are high levels of *miR156* but reduced levels of *SPL9* and *miR172*, whereas an increased accumulation of *miR156* and *miR172* in SD-induced stolons reflects a lack of regulation of *miR172* by *miR156*, possibly due to the tissue-specific action of *miR156* or spatial exclusion.

Several interesting observations regarding the effect of *miR156* on tuberization were noted in our study. In stolons (the tissue destined to form a tuber) harvested from SD-induced wild-type plants, an approximately 8-fold increase in the level of *miR156* was detected (Fig. 1E). Also, *miR156* OE lines, when incubated under SD conditions, produced aerial tubers, as reported in a recent work (Eviatar-Ribak et al., 2013). However, in our study, *miR156* OE lines exhibited a reduction in overall tuber yield and the levels of the tuberization markers *miR172* and *StSP6A* (Fig. 4, D–F). Considering these observations, should *miR156* be termed as an activator or a repressor of tuberization? If *miR156* acts as an activator, *miR156* OE lines would have produced tubers under LD (noninductive) conditions, as observed previously for StBEL5 (Banerjee et al., 2006a), *miR172* (Martin et al., 2009), and StSP6A (Navarro et al., 2011) OE lines. In our study, *miR156* OE lines produced aerial tubers in SD conditions (Fig. 4B). This rules out the possibility of *miR156* functioning as a repressor. The reduced levels of tuberization markers in *miR156* OE lines can possibly be due to the prolonged juvenile phase of these plants, which in turn reduced the overall tuber yield. In potato, all axillary meristems have the capacity to form tubers, and under permissive conditions any meristem can produce aerial tubers. However, this potential is suppressed except in stolons (Xu et al., 1998). We propose that under tuber-inductive conditions, a threshold level of *miR156* facilitates tuber formation from a meristem. Overexpression of *miR156* in potato results in levels above threshold in all the axillary meristems; hence, the plant produces aerial tubers under SD conditions. The recent work by Eviatar-Ribak and coworkers (2013) demonstrated that *TLOG1* OE tomato plants produced sessile tubers only in basal meristems, whereas *TLOG1-miR156* double OE plants produced sessile tubers from all axillary meristems. In our study, we used potato subspecies *andigena*, which is sensitive to photoperiod for tuberization. When *miR156* is overexpressed in this background, the OE plants produced aerial tubers only under SD conditions, whereas in LD conditions, the axillary meristems produced only branches. This observation clearly established that increased levels of *miR156* in OE plants alone are not sufficient for tuber formation but that tuber-inductive conditions are required for aerial tuber formation.

miR156 as a Potential Phloem-Mobile Long-Distance Signal

The detection of *miR156* in LMPC-harvested phloem cells and an increased accumulation in phloem exudates under SD photoperiod suggest that *miR156* could possibly act as a long-distance signal in potato development. Our grafting assays support this hypothesis, as increased levels of mature *miR156* could be detected in the stock stems of SD-induced heterografts (Fig. 9E). Further molecular analysis ruled out the possibility of *miR156a* precursor transgene movement (Fig. 9F; Supplemental Fig. S8, A–D). In addition, morphological changes in leaves and trichome phenotypes further support *miR156* transport. Reverse graft assays showed that the mobility of *miR156* was restricted to a shoot-to-root direction. Questions could be raised. Is *miR156* transported as a double-stranded or single-stranded form in the phloem? The presence of the *miR156** strand in potato phloem sap indicates that it is possibly transported as a *miR156*/*miR156** duplex. Similar to our results, previous studies (Buhtz et al., 2008, 2010; Pant et al., 2008; Hsieh et al., 2009) also reported the presence of a star strand along with the mature miRNA in the phloem stream. Another explanation for *miR156** in potato phloem could be its association with the RNA-induced silencing complex to target different genes. miRNA* species are reported to be associated with Argonaut proteins and to have inhibitory effects on target gene expression in *Drosophila* species (Okamura et al., 2008). A recent report by Devers and coworkers (2011) described a similar phenomenon in *Medicago truncatula* roots. Although a handful of miRNAs have now been detected in phloem of several plant species such as pumpkin (Yoo et al., 2004), Arabidopsis (Varkonyi-Gasic et al., 2010), and *Brassica* (Buhtz et al., 2008), only three miRNAs, *miR399*, *miR395*, and *miR172* (Pant et al., 2008; Buhtz et al., 2010; Kasai et al., 2010), were demonstrated to act as long-distance mobile signals. We show that *miR156* is involved in the regulation of plant architecture and tuberization and might be another miRNA to be transported via the phloem over long distances. The availability of techniques to differentiate between mature endogenous miRNAs from transgenic miRNAs would perhaps provide the final evidence for miRNA mobility.

Based on our results, we propose a model for the regulation of tuberization by *miR156*. We hypothesize that under tuber-inductive (SD) conditions, *miR156* is transported to stolons through the phloem, accumulates in underground stolons (which in turn reduces the *miR156* accumulation in leaves and stems), and facilitates underground tuber formation. Reduced *miR156* accumulation in aerial organs inhibits the formation of aerial tubers, whereas in LD conditions, increased levels of *miR156* in leaves and stems assist the vegetative growth of the plant. *miR156* exerts this effect presumably through a *miR156*-SPL9-*miR172* regulatory module and possibly arrests tuberization under LD conditions. It appears that *miR156* has a different function in SD and LD photoperiods. We also cannot rule out the possibility that the high accumulation of *miR156* in SD-induced stolons is associated with controlling tuber transitions, the maintenance of the juvenile phase, or even tuber dormancy. Future work will help to elucidate the additional functions of *miR156* in potato.

MATERIALS AND METHODS

Plant Material and Growth Conditions

In this study, potato (*Solanum tuberosum* subspecies *andigena* 7540) was used. This is a photoperiod-responsive plant that tuberizes under SD conditions (8 h of light) and does not produce tubers under LD conditions (16 h of light). In vitro plants were grown under LD conditions at 25°C in a growth incubator (Percival Scientific). Soil plants were grown at 22°C under LD photoperiod in environmental chambers (Percival Scientific). For age-specific expression studies of *miR156*, tissue culture-raised plants were transferred to soil and incubated up to 14 weeks. Tissues (fully expanded mature leaves and stem) were collected after specific time intervals (2, 7, 12, 13, and 14 weeks) and stored at −80°C until further use. For photoperiod-dependent expression studies, plants were induced under both SD and LD conditions in environmental chambers for 15 d. Different tissues (leaf, stem, stolon, and swollen stolon) were harvested after 15 dpi. For quantifying *miR156* levels in 0-, 15-, and 30-d-old tubers stored post harvest (tuber dormancy), tuber eyes were isolated and stored at −80°C. In the case of tobacco (*Nicotiana tabacum* cv Petit Havana), plants were grown under LD conditions in environmental chambers.

Validation of *miR156*

Total RNA was harvested from mature leaves and stem tissue of potato, and *StmiR156a* (BI432985.1) precursor was amplified by RT-PCR (details of all the primers and accession numbers are given in Supplemental Tables S3 and S4). The amplicon was then sequence confirmed. Mature *miR156* was detected by stem-loop RT-PCR as described earlier (Varkonyi-Gasic et al., 2007). Total RNA was isolated by TRIzol reagent (Invitrogen) following the manufacturer's instructions. RT was carried out using stem-loop primer miR156STP. End-point PCR was performed using miR156FP and universal reverse primer (univRP). The 61-bp amplicon was cloned in the subcloning vector pGEM-T Easy (Promega) and was confirmed by sequencing.

Analysis of miRNA Levels

In the entire study, levels of miRNAs (*miR156* and *miR172*) were determined by stem-loop qRT-PCR. One microgram of total RNA was used for all RT reactions except for the quantification of miRNAs from phloem sap, where 100 ng of RNA was used. Stem-loop reverse primers miR156STP and miR172STP were used for *miR156* and *miR172*, respectively. RT was carried out as per a previous protocol (Varkonyi-Gasic et al., 2007). Quantitative PCR (qPCR) for *miR156* (miR156FP and univRP) and *miR172* (miR172FP and univRP) was performed in a Mastercycler ep realplex (Eppendorf). For normalization, 5S ribosomal RNA was reverse transcribed by stem-loop primer 5S rRNASTP and amplified by 5S rRNAFP and univRP. All the PCRs were incubated at 95°C for 5 min followed by 40 cycles of 95°C for 5 s, 60°C for 10 s, and 68°C for 8 s. PCR specificity was checked by melting curve analysis, and data were analyzed using the $2^{-\Delta\Delta Ct}$ method (Livak and Schmittgen, 2001).

Construct Design and Plant Transformation

To generate *miR156* OE lines of potato, the precursor sequence (*StmiR156a*; BI432985.1) of *miR156* was amplified from total RNA harvested from leaves using the primers miR156preFP and miR156preRP. The PCR product was digested with *Xba*I-*Sac*I and cloned into the binary vector pBI121 under the control of the CaMV 35S promoter. This construct was then mobilized into *Agrobacterium tumefaciens* strain GV2260. Transgenic plants were generated following the protocol by Banerjee et al. (2006b). *miR156* OE lines of tobacco were raised as described by Horsch et al. (1985). Kanamycin-resistant transgenic plants were selected for further analysis and were maintained in Murashige and

Skoog basal medium (Murashige and Skoog, 1962) until further use, whereas rSPL9 transgenic lines were generated by introducing silent mutations in the MRE. Mutations were incorporated by site-directed mutagenesis using Turbo DNA polymerase (Stratagene). The primers used for site-directed mutagenesis in MRE were rSPL9FP and rSPL9RP. Amplification of rSPL9 was carried out by using primer pair SPL9FP and SPL9RP3, and it was cloned in binary vector pBI121 downstream of the CaMV 35S promoter. Transgenic plants of rSPL9 were generated and maintained as described above.

Leaf and Stem Histology

For histology, a modified protocol of Cai and Lashbrook (2006) was followed. Briefly, leaves and stems of 8-week-old plants (the wild type and *miR156* OE lines 5.1 and 6.2) grown under LD conditions were fixed in chilled ethanol:acetic acid (3:1; Merck). The tissues were vacuum infiltrated (400 mm of mercury) for 30 min and then stored at 4°C overnight. Fixed tissues were then dehydrated at room temperature in a graded series of ethanol (75% [v/v], 95% [v/v], and 100% [v/v] ethanol) followed by washes of a combination of ethanol and xylene series. Tissue blocks were prepared with molten Paraplast (Leica). Ten-micrometer sections were cut by a microtome (Leica) and placed on glass slides. Dried slides were deparaffinized by washing twice in 100% xylene and were observed with a microscope.

Environmental Mode Scanning Electron Microscopy of Leaves

Leaves of 8-week-old plants (the wild type and *miR156* OE lines 5.1 and 6.2) grown under LD conditions were used for scanning electron microscopy in the environmental mode (eSEM) with a Quanta 200 3D eSEM apparatus (FEI), and leaf morphology was documented.

Analysis of Tuberization

Both wild-type and *miR156* OE lines were grown in soil at 22°C under LD conditions in environmental chambers for 3 weeks. Thereafter, 10 plants each were shifted to SD and LD conditions and were incubated further for 4 weeks. To analyze *StSP6A* and *miR172* levels in these plants, leaf tissues were harvested 8 dpi from both of these lines. *miR172* levels were also quantified in 15-d post SD-induced stolons of wild-type and *miR156* OE plants (line 5.1). The tuberization phenotype was scored after 4 weeks of induction.

Analysis of Zeatin Riboside and Orobanchyl Acetate by HR-MS

Axillary meristems were harvested from wild-type and *miR156* OE 5.1 plants induced for 15 d in LD and SD conditions and ground in liquid nitrogen. For HR-MS analysis, a modified protocol of Forcat et al. (2008) was followed. One hundred milligrams of tissue was used for extraction in 400 μL of 10% (v/v) methanol and 1% (v/v) glacial acetic acid. This mixture was vigorously vortexed and stored on ice for 2 h, followed by centrifugation to obtain the supernatant. This was repeated three times, and the volume of the supernatant was adjusted to 2 mL in a volumetric flask. Samples were resolved through a Thermo Scientific Hypersil Gold column of particle size 5 μm with a flow rate of 0.5 mL min^{-1} and a gradient solvent program of 25 min (0 min, 10% methanol-water; 0.5 min, 10% methanol-water; 3 min, 45% methanol-water; 20 min, 50% methanol-water; 22 min, 90% methanol-water; 23 min, 10% methanol-water; 25 min, 10% methanol-water). Formic acid (0.1%; liquid chromatography-mass spectrometry grade) was also added to methanol and water. Mass spectrometry and tandem mass spectrometry experiments were performed in electrospray ionization-positive ion mode using the tune method as followed: sheath gas flow rate, 45 units N_2; auxiliary gas flow rate, 10 units N_2; sweep gas flow rate, 2 units N_2; spray voltage, 3.60 kV; spray current, 3.70 μA; capillary temperature, 320°C; source lens R_F level, 50; heater temperature, 350°C. Electrospray ionization-mass spectrometry data were recorded in full scan mode within the mass-to-charge ratio range 100 to 1,000. A standard curve for quantification was prepared using zeatin riboside (Sigma). Orobanchyl acetate was identified based on mass spectrometry analysis, and quantification was performed considering the peak areas.

Analysis of *StSP6A*, *StLOG1*, and *StCyclin D3.1*

One microgram of total RNA was used for *StSP6A* analysis from 8-d-old SD-induced leaves of wild-type and *miR156* OE line plants. 18S ribosomal RNA (50 ng) was used for normalization. For RT-PCR, the SuperScript III one-step RT-PCR system with platinum Taq DNA polymerase (Invitrogen) was used as per the manufacturer's instructions. Semiquantitative RT-PCR for *StSP6A* was performed using the following primers: SP6AFP and SP6ARP. RT-PCR conditions were as follows: 50°C for 30 min, 94°C for 2 min, followed by 25 cycles of 94°C 15 s, 55°C for 15 s, and 68°C for 1 min. The cycle number for 18S RNA was restricted to 10, while the program remained the same as for *StSP6A*. For analysis of *StLOG1* and *StCyclin D3.1*, total RNA was isolated from axillary meristems of wild-type and *miR156* OE 5.1 plants grown in SD photoperiod for 15 d by TRIzol reagent. One microgram of total RNA was used for complementary DNA (cDNA) synthesis by SuperScript III reverse transcriptase (Invitrogen) using an oligo(dT) primer. qPCR was performed on a Mastercycler ep realplex with LOG1FP-LOG1RP and CyclinFP-CyclinRP. The reactions were carried out using KAPA SYBR green master mix (Kapa Biosystems) and incubated at 95°C for 2 min followed by 40 cycles of 95°C for 15 s and 60°C for 30 s. Glyceraldehyde 3 phosphate dehydrogenase was used for normalization for all the reactions. PCR specificity was checked by melting curve analysis, and data were analyzed using the $2^{-\Delta\Delta Ct}$ method (Livak and Schmittgen, 2001).

Prediction of *miR156* Targets

miR156 targets in potato were predicted using bioinformatic tools. To increase the efficiency of target prediction, psRNATarget (plantgrn.noble.org/psRNATarget/; Dai and Zhao, 2011) and TargetAlign (leonxie.com/targetAlign.php; Xie and Zhang, 2010) online tools were used. Based on their score and consistency of results, five sequences were short listed as potential *miR156* targets. These targets showed homology (40%–80%) with AtSPL3, AtSPL6, AtSPL9, AtSPL13, and RcoLG1 (for *Ricinus communis* LIGULELESS1) and were termed StSPL3, StSPL6, StSPL9, StSPL13, and StLG1, respectively. Their coding sequences were retrieved from the Online Resource for Community Annotation of Eukaryotes (http://bioinformatics.psb.ugent.be/orcae/; Sterck et al., 2012) and the Database of Plant Transcription Factors (http://planttfdb.cbi.edu.cn/; Zhang et al., 2011a).

Cleavage Site Mapping

To validate the candidate targets of *miR156* in planta, modified RLM 5′ RACE was performed using the First Choice RLM-RACE kit (Ambion). Total RNA was extracted from wild-type potato leaves by TRIzol reagent and was directly ligated to RNA adaptor without any enzymatic pretreatments. cDNA synthesis was performed using the respective gene-specific reverse primers. Two rounds of PCR were conducted with adaptor-specific forward primers and gene-specific reverse primers (SPL3, SPL3RP1-SPL3RP2; SPL6, SPL6RP1-SPL6RP2; SPL9, SPL9RP1-SPL9RP2; SPL13, SPL13RP1-SPL13RP2; LG1, LG1RP1-LG1RP2). Amplicons were then cloned into the subcloning vector pGEM-T Easy and were sequenced to identify the miRNA cleavage sites.

Analysis of *StSPLs*

Total RNA from wild-type and *miR156* OE plants was isolated by TRIzol reagent as per the manufacturer's instructions. One microgram of total RNA was reverse transcribed using gene-specific primers by Moloney murine leukemia virus reverse transcriptase (Promega). For normalization, *GAPDH* was reverse transcribed. The primers used for reverse transcription were SPL3RP2, SPL6RP2, SPL9RP2, SPL13RP2, LG1RP2, and GAPDHRP. qPCR was performed on a Mastercycler ep realplex with the same reverse primers mentioned above. Forward primers were SPL3qFP, SPL6qFP, SPL9qFP, SPL13qFP, LG1qFP, and GAPDHFP. The reactions were carried out using the KAPA SYBR green master mix and incubated at 95°C for 2 min followed by 40 cycles of 95°C for 15 s, 52°C for 15 s, and 60°C for 20 s. For *GAPDH*, all conditions were similar, but the annealing temperature was 55°C. For StLG1, all conditions were similar except that the extension time was 10 s. PCR specificity was checked by melting curve analysis, and data were analyzed using the $2^{-\Delta\Delta Ct}$ method (Livak and Schmittgen, 2001).

Gel Retardation Assay

A 6× His-tagged fusion construct was generated by introducing the 1,152-bp coding sequence of StSPL9 in frame into the pET28a expression vector and transformed into *Escherichia coli* BL21 (DE3) cells. Cells were grown at 37°C until the optical density at 600 nm reached 0.6, induced with 1.0 mM isopropyl-β-D-thiogalactopyranoside, and cultured for 3 h at 37°C. The cells were lysed

by sonication. The tagged protein was purified using nickel-nitrilotriacetic acid agarose beads. Purified StSPL9 protein aliquots were frozen in liquid N_2 and stored at −80°C. Four overlapping fragments of the MIR172b promoter were used for gel mobility shift assays. Promoter fragments were PCR amplified from potato genomic DNA and were purified on columns. The respective primer sequences are provided in Supplemental Table S3. The 5′ ends of the fragments were then labeled with γ-^{32}P using the KinaseMax kit (Ambion). The DNA-binding reactions were set up at 24°C in 20 μL containing 10 mM Tris-HCl (pH 7.5), 5% glycerol, 0.5 mM EDTA, 0.5 mM dithiothreitol, 0.05% Nonidet P-40, 50 mM NaCl, 50 mg L^{-1} poly(dG-dC), 250 ng of protein, and 1 fmol of labeled DNA. After incubation at 24°C for 60 min, the reactions were resolved on a 6% native polyacrylamide gel in 1× Tris-borate-EDTA buffer. The gel was dried and exposed to x-ray film. In the cold competition assays, 100-fold more unlabeled double-stranded DNA fragment (P1) was added to the reaction and loaded onto the gel every 15 min.

Detection of *miR156* in the Phloem

Stem sections of 12-week-old wild-type plants were fixed as described above in the histology section. LMPC-mediated harvest of phloem cells (Carl Zeiss PALM laser micro beam) and RNA extraction from these cells were done as per Yu et al. (2007). Total RNA was extracted using TRIzol reagent. Mature *miR156* and *miR156** were detected by stem-loop RT-PCR as described earlier. Primer sequences for *miR156** are provided in Supplemental Table S3.

For analysis of the differential accumulation of *miR156* in phloem sap of SD- and LD-grown wild-type plants, sap extraction and RNA isolation were done as per Campbell et al. (2008) with a minor modification (the phloem exudate was harvested at 18°C). Sap collection was performed at 8, 15, and 30 dpi. To assess the purity of phloem sap, RT-PCR was performed for nitrate transporter (root-specific transcript) and G2-like transcription factor (phloem-specific transcript) using 150 ng of RNA as mentioned before (Banerjee et al., 2006a). The SuperScript III one-step RT-PCR system with platinum Taq DNA polymerase was used as per the manufacturer's instructions. For nitrate transporter, RT-PCR conditions were as follows: 55°C for 30 min, 94°C for 2 min, followed by 40 cycles of 94°C for 15 s, 50°C for 30 s, and 68°C for 1 min, with a final extension at 68°C for 5 min. For G2-like transcription factor, all conditions were similar except that annealing was at 56°C and extension was for 30 s. To quantify *miR156* levels in phloem sap, 100 ng of total RNA was used for *miR156*-specific stem-loop qRT-PCR as described above, except that the cycle number was increased to 50. qRT-PCR cycle threshold (Ct) value differences were calculated for *miR156* accumulation and plotted as described previously (Pant et al., 2008).

Soil-Grown Heterografts

Wild-type and *miR156* OE lines were maintained in an environmental chamber until grafting was performed. Grafts were made with wild-type and *miR156* OE transgenic potato plants as per our previous protocol (Mahajan et al., 2012). *miR156* OE lines were used as scions and wild-type plants as stock (heterografts), while for reverse grafting, *miR156* OE plants served as stock and wild-type plants as scion (reverse grafts). Homografts (wild type on wild type) were used as controls in both cases. Equal numbers (10 each) of heterografts, reverse grafts, and homografts were made and maintained in environmental chambers for hardening for 4 weeks. Hardened grafts were further incubated in SD conditions for 4 weeks. Scion and stock samples (devoid of graft union) were harvested, and phenotypes such as leaf number, trichomes, and axillary branches were scored. qRT-PCR was performed for *miR156* accumulation in both heterograft stock samples and reverse graft scion samples with respective tissues from homografts as controls. Tuberization phenotypes were scored for all grafts.

For *miR156a* precursor transgene detection, RT-PCR was performed by the SuperScript III one-step RT-PCR system with platinum Taq DNA polymerase using 250 ng of total RNA. The primers used were miR156pre FP and transgene-specific NOST RP. The RT-PCR conditions were as follows: 50°C for 30 min, 94°C for 2 min, followed by 35 cycles of 94°C for 15 s, 50°C for 15 s, and 68°C for 1 min, with a final extension of 68°C for 5 min.

For comparative analysis of *miR156* (mature) and *miR156a* precursor levels in wild-type and grafted plants, 500 ng of RNA was used. Stem-loop qRT-PCR of *miR156* (mature) was performed as described above. For *miR156a* precursor quantification, cDNA synthesis was performed using oligo(dT) and SuperScript III reverse transcriptase enzyme. qPCR was performed on a Mastercycler ep realplex with miR156preFP and miR156preRP primers. The reactions were carried out using KAPA SYBR green master mix and incubated at 95°C for 2 min followed by 40 cycles of 95°C for 15 s, 50°C for 10 s, and 72°C for 18s. GAPDH was used for normalization. PCR specificity was checked by melting curve analysis, and data were analyzed using the $2^{-\Delta\Delta Ct}$ method (Livak and Schmittgen, 2001).

Sequence data from this article can be found in the GenBank/EMBL data libraries under accession numbers BI432985.1 (miR156a precursor), AC237992 (MIR172b promoter), CK267169.1 (NT), CK853924.1 (G2), in the Online Resource for Community Annotation of Eukaryotes (ORCAE) under accession numbers sotub10g009340 (SPL3), sotub12g015890 (SPL6), sotub10g020210 (SPL9), sotub05g016640 (SPL13), sotub05g016440 (LG1), and in the Potato Genome Sequencing Consortium under accession numbers: PGSC0003DMG400023365 (SP6A), PGSC0003DMT400009551 (LOG1), PGSC0003DMT400064307 (Cyclin D3.1), PGSC chr07:1782100..1784700 (MIR156a promoter).

Supplemental Data

The following materials are available in the online version of this article.

Supplemental Figure S1. *miR156* overexpression in potato.

Supplemental Figure S2. Overexpression of *miR156* in tobacco.

Supplemental Figure S3. HR-MS of zeatin riboside.

Supplemental Figure S4. Mass spectrum of zeatin riboside.

Supplemental Figure S5. HR-MS of orobanchyl acetate.

Supplemental Figure S6. Mass spectrum of orobanchyl acetate.

Supplemental Figure S7. Overexpression of rSPL9 in potato.

Supplemental Figure S8. Comparative analysis of *miR156* (mature) and *miR156a* precursor levels in wild-type and grafted plants.

Supplemental Table S1. Detailed analysis of *miR156* targets in potato.

Supplemental Table S2. Potential light regulatory elements present in the upstream sequence of *miR156a*.

Supplemental Table S3. List of primers.

Supplemental Table S4. List of accession numbers.

ACKNOWLEDGMENTS

We thank David J. Hannapel (Iowa State University) and Julia Kehr (University of Hamburg) for their critical reading of the manuscript, the director, National Chemical Laboratory, for providing us the eSEM facilities, Sanjeev Galande (Indian Institute of Science Education and Research) for his help in the gel retardation assays, and Saikat Haldar (National Chemical Laboratory) for his technical help in carrying out HR-MS analysis.

Received October 18, 2013; accepted December 13, 2013; published December 18, 2013.

LITERATURE CITED

Atkins CA, Smith PMC, Rodriguez-Medina C (2011) Macromolecules in phloem exudates: a review. Protoplasma **248:** 165–172

Axtell MJ, Bowman JL (2008) Evolution of plant microRNAs and their targets. Trends Plant Sci **13:** 343–349

Banerjee AK, Chatterjee M, Yu Y, Suh SG, Miller WA, Hannapel DJ (2006a) Dynamics of a mobile RNA of potato involved in a long-distance signaling pathway. Plant Cell **18:** 3443–3457

Banerjee AK, Prat S, Hannapel DJ (2006b) Efficient production of transgenic potato (*S. tuberosum* L. ssp. *andigena*) plants via *Agrobacterium tumefaciens*-mediated transformation. Plant Sci **170:** 732–738

Birkenbihl RP, Jach G, Saedler H, Huijser P (2005) Functional dissection of the plant-specific SBP-domain: overlap of the DNA-binding and nuclear localization domains. J Mol Biol **352:** 585–596

Buhtz A, Pieritz J, Springer F, Kehr J (2010) Phloem small RNAs, nutrient stress responses, and systemic mobility. BMC Plant Biol **10:** 64

Buhtz A, Springer F, Chappell L, Baulcombe DC, Kehr J (2008) Identification and characterization of small RNAs from the phloem of *Brassica napus*. Plant J **53:** 739–749

Cai S, Lashbrook CC (2006) Laser capture microdissection of plant cells from tape-transferred paraffin sections promotes recovery of structurally intact RNA for global gene profiling. Plant J **48:** 628–637

Campbell BA, Hallengren J, Hannapel DJ (2008) Accumulation of BEL1-like transcripts in solanaceous species. Planta **228:** 897–906

Carlsbecker A, Lee JY, Roberts CJ, Dettmer J, Lehesranta S, Zhou J, Lindgren O, Moreno-Risueno MA, Vatén A, Thitamadee S, et al (2010) Cell signalling by microRNA165/6 directs gene dose-dependent root cell fate. Nature **465:** 316–321

Chen X, Zhang Z, Liu D, Zhang K, Li A, Mao L (2010) SQUAMOSA promoter-binding protein-like transcription factors: star players for plant growth and development. J Integr Plant Biol **52:** 946–951

Chuck G, Cigan AM, Saeteurn K, Hake S (2007) The heterochronic maize mutant Corngrass1 results from overexpression of a tandem microRNA. Nat Genet **39:** 544–549

Chuck G, O'Connor D (2010) Small RNAs going the distance during plant development. Curr Opin Plant Biol **13:** 40–45

Corbesier L, Vincent C, Jang S, Fornara F, Fan Q, Searle I, Giakountis A, Farrona S, Gissot L, Turnbull C, et al (2007) FT protein movement contributes to long-distance signaling in floral induction of *Arabidopsis*. Science **316:** 1030–1033

Dai X, Zhao PX (2011) psRNATarget: a plant small RNA target analysis server. Nucleic Acids Res **39:** W155–W159

Devers EA, Branscheid A, May P, Krajinski F (2011) Stars and symbiosis: microRNA- and microRNA*-mediated transcript cleavage involved in arbuscular mycorrhizal symbiosis. Plant Physiol **156:** 1990–2010

Domagalska MA, Leyser O (2011) Signal integration in the control of shoot branching. Nat Rev Mol Cell Biol **12:** 211–221

Eviatar-Ribak T, Shalit-Kaneh A, Chappell-Maor L, Amsellem Z, Eshed Y, Lifschitz E (2013) A cytokinin-activating enzyme promotes tuber formation in tomato. Curr Biol **23:** 1057–1064

Forcat S, Bennett MH, Mansfield JW, Grant MR (2008) A rapid and robust method for simultaneously measuring changes in the phytohormones ABA, JA and SA in plants following biotic and abiotic stress. Plant Methods **4:** 16–23

Fu C, Sunkar R, Zhou C, Shen H, Zhang JY, Matts J, Wolf J, Mann DGJ, Stewart CN Jr, Tang Y, et al (2012) Overexpression of miR156 in switchgrass (*Panicum virgatum L.*) results in various morphological alterations and leads to improved biomass production. Plant Biotechnol J **10:** 443–452

Gandikota M, Birkenbihl RP, Höhmann S, Cardon GH, Saedler H, Huijser P (2007) The miRNA156/157 recognition element in the 3′ UTR of the *Arabidopsis* SBP box gene SPL3 prevents early flowering by translational inhibition in seedlings. Plant J **49:** 683–693

Gomez-Roldan V, Fermas S, Brewer PB, Puech-Pagès V, Dun EA, Pillot JP, Letisse F, Matusova R, Danoun S, Portais JC, et al (2008) Strigolactone inhibition of shoot branching. Nature **455:** 189–194

Gou JY, Felippes FF, Liu CJ, Weigel D, Wang JW (2011) Negative regulation of anthocyanin biosynthesis in *Arabidopsis* by a miR156-targeted SPL transcription factor. Plant Cell **23:** 1512–1522

Griffiths-Jones S, Saini HK, van Dongen S, Enright AJ (2008) miRBase: tools for microRNA genomics. Nucleic Acids Res **36:** D154–D158

Harper L, Freeling M (1996) Interactions of liguleless1 and liguleless2 function during ligule induction in maize. Genetics **144:** 1871–1882

Haywood V, Yu TS, Huang NC, Lucas WJ (2005) Phloem long-distance trafficking of GIBBERELLIC ACID-INSENSITIVE RNA regulates leaf development. Plant J **42:** 49–68

Higo K, Ugawa Y, Iwamoto M, Korenaga T (1999) Plant cis-acting regulatory DNA elements (PLACE) database: 1999. Nucleic Acids Res **27:** 297–300

Horsch RB, Rogers SG, Fraley RT (1985) Transgenic plants. Cold Spring Harb Symp Quant Biol **50:** 433–437

Hsieh LC, Lin SI, Shih AC, Chen JW, Lin WY, Tseng CY, Li WH, Chiou TJ (2009) Uncovering small RNA-mediated responses to phosphate deficiency in Arabidopsis by deep sequencing. Plant Physiol **151:** 2120–2132

Huijser P, Schmid M (2011) The control of developmental phase transitions in plants. Development **138:** 4117–4129

Jackson SD (2009) Plant responses to photoperiod. New Phytol **181:** 517–531

Jackson SD, James P, Prat S, Thomas B (1998) Phytochrome B affects the levels of a graft-transmissible signal involved in tuberization. Plant Physiol **117:** 29–32

Jiao Y, Wang Y, Xue D, Wang J, Yan M, Liu G, Dong G, Zeng D, Lu Z, Zhu X, et al (2010) Regulation of OsSPL14 by OsmiR156 defines ideal plant architecture in rice. Nat Genet **42:** 541–544

Kasai A, Kanehira A, Harada T (2010) *miR172* can move long distance in *Nicotiana benthamiana*. The Open Plant Sci J **4:** 1–6

Kehr J, Buhtz A (2008) Long distance transport and movement of RNA through the phloem. J Exp Bot **59:** 85–92

Kehr J, Buhtz A (2013) Endogenous RNA constituents of the phloem and their possible roles in long-distance signaling. *In* GA Thompson, AJE van Bel, eds, Phloem: Molecular Cell Biology, Systemic Communication, Biotic Interactions. Wiley-Blackwell Publishing, Oxford, pp 186–208

Kim M, Canio W, Kessler S, Sinha N (2001) Developmental changes due to long-distance movement of a homeobox fusion transcript in tomato. Science **293:** 287–289

Kurakawa T, Ueda N, Maekawa M, Kobayashi K, Kojima M, Nagato Y, Sakakibara H, Kyozuka J (2007) Direct control of shoot meristem activity by a cytokinin-activating enzyme. Nature **445:** 652–655

Lee J, Park JJ, Kim SL, Yim J, An G (2007) Mutations in the rice liguleless gene result in a complete loss of the auricle, ligule, and laminar joint. Plant Mol Biol **65:** 487–499

Lin T, Sharma P, Gonzalez DH, Viola IL, Hannapel DJ (2013) The impact of the long-distance transport of a *BEL1*-like messenger RNA on development. Plant Physiol **161:** 760–772

Livak KJ, Schmittgen TD (2001) Analysis of relative gene expression data using real-time quantitative PCR and the $2^{-\Delta\Delta CT}$ method. Methods **25:** 402–408

Mahajan A, Bhogale S, Kang IH, Hannapel DJ, Banerjee AK (2012) The mRNA of a Knotted1-like transcription factor of potato is phloem mobile. Plant Mol Biol **79:** 595–608

Marín-González E, Suárez-López P (2012) "And yet it moves": cell-to-cell and long-distance signaling by plant microRNAs. Plant Sci **196:** 18–30

Martin A, Adam H, Díaz-Mendoza M, Zurczak M, González-Schain ND, Suárez-López P (2009) Graft-transmissible induction of potato tuberization by the microRNA miR172. Development **136:** 2873–2881

Martinez-Garcia JF, Virgos-Soler A, Prat S (2002) Control of photoperiodregulated tuberization in potato by the Arabidopsis flowering-time gene CONSTANS. PNAS **99:** 15211–15216

Miyashima S, Koi S, Hashimoto T, Nakajima K (2011) Non-cell-autonomous microRNA165 acts in a dose-dependent manner to regulate multiple differentiation status in the *Arabidopsis* root. Development **138:** 2303–2313

Molnar A, Melnyk CW, Bassett A, Hardcastle TJ, Dunn R, Baulcombe DC (2010) Small silencing RNAs in plants are mobile and direct epigenetic modification in recipient cells. Science **328:** 872–875

Murashige T, Skoog F (1962) A revised medium for rapid growth and bioassays with tobacco tissue cultures. Physiol Plant **15:** 473–497

Navarro C, Abelenda JA, Cruz-Oró E, Cuéllar CA, Tamaki S, Silva J, Shimamoto K, Prat S (2011) Control of flowering and storage organ formation in potato by FLOWERING LOCUS T. Nature **478:** 119–122

Nodine MD, Bartel DP (2010) MicroRNAs prevent precocious gene expression and enable pattern formation during plant embryogenesis. Genes Dev **24:** 2678–2692

Okamura K, Phillips MD, Tyler DM, Duan H, Chou YT, Lai EC (2008) The regulatory activity of microRNA* species has substantial influence on microRNA and 3′ UTR evolution. Nat Struct Mol Biol **15:** 354–363

Pant BD, Buhtz A, Kehr J, Scheible WR (2008) MicroRNA399 is a long-distance signal for the regulation of plant phosphate homeostasis. Plant J **53:** 731–738

Schwab R, Palatnik JF, Riester M, Schommer C, Schmid M, Weigel D (2005) Specific effects of microRNAs on the plant transcriptome. Dev Cell **8:** 517–527

Shikata M, Koyama T, Mitsuda N, Ohme-Takagi M (2009) *Arabidopsis* SBP-box genes SPL10, SPL11 and SPL2 control morphological change in association with shoot maturation in the reproductive phase. Plant Cell Physiol **50:** 2133–2145

Sterck L, Billiau K, Abeel T, Rouzé P, Van de Peer Y (2012) ORCAE: online resource for community annotation of eukaryotes. Nat Methods **9:** 1041

Tomato Genome Consortium (2012) The tomato genome sequence provides insights into fleshy fruit evolution. Nature **485:** 635–641

Usami T, Horiguchi G, Yano S, Tsukaya H (2009) The more and smaller cells mutants of *Arabidopsis thaliana* identify novel roles for SQUAMOSA

PROMOTER BINDING PROTEIN-LIKE genes in the control of heteroblasty. Development **136:** 955–964

Varkonyi-Gasic E, Gould N, Sandanayaka M, Sutherland P, MacDiarmid RM (2010) Characterisation of microRNAs from apple (*Malus domestica* 'Royal Gala') vascular tissue and phloem sap. BMC Plant Biol **10:** 159

Varkonyi-Gasic E, Wu R, Wood M, Walton EF, Hellens RP (2007) Protocol: a highly sensitive RT-PCR method for detection and quantification of microRNAs. Plant Methods **3:** 12

Vauterin M, Frankard V, Jacobs M (1999) The *Arabidopsis thaliana* dhdps gene encoding dihydrodipicolinate synthase, key enzyme of lysine biosynthesis, is expressed in a cell-specific manner. Plant Mol Biol **39:** 695–708

Vorst O, van Dam F, Oosterhoff-Teertstra R, Smeekens S, Weisbeek P (1990) Tissue-specific expression directed by an *Arabidopsis thaliana* preferredoxin promoter in transgenic tobacco plants. Plant Mol Biol **14:** 491–499

Waksman G, Lebrun M, Freyssinet G (1987) Nucleotide sequence of a gene encoding sunflower ribulose-1,5-bisphosphate carboxylase/oxygenase small subunit (rbcs). Nucleic Acids Res **15:** 7181

Wang JW, Park MY, Wang LJ, Koo Y, Chen XY, Weigel D, Poethig RS (2011) miRNA control of vegetative phase change in trees. PLoS Genet **7:** e1002012

Waterhouse PM, Wang MB, Lough T (2001) Gene silencing as an adaptive defence against viruses. Nature **411:** 834–842

Wu G, Park MY, Conway SR, Wang JW, Weigel D, Poethig RS (2009) The sequential action of miR156 and miR172 regulates developmental timing in *Arabidopsis*. Cell **138:** 750–759

Wu G, Poethig RS (2006) Temporal regulation of shoot development in Arabidopsis thaliana by miR156 and its target SPL3. Development **133:** 3539–3547

Xie F, Frazier TP, Zhang B (2011) Identification, characterization and expression analysis of microRNAs and their targets in the potato (*Solanum tuberosum*). Gene **473:** 8–22

Xie F, Zhang B (2010) Target-align: a tool for plant microRNA target identification. Bioinformatics **26:** 3002–3003

Xie K, Shen J, Hou X, Yao J, Li X, Xiao J, Xiong L (2012) Gradual increase of miR156 regulates temporal expression changes of numerous genes during leaf development in rice. Plant Physiol **158:** 1382–1394

Xie K, Wu C, Xiong L (2006) Genomic organization, differential expression, and interaction of SQUAMOSA promoter-binding-like transcription factors and microRNA156 in rice. Plant Physiol **142:** 280–293

Xing S, Salinas M, Höhmann S, Berndtgen R, Huijser P (2010) miR156-targeted and nontargeted SBP-box transcription factors act in concert to secure male fertility in *Arabidopsis*. Plant Cell **22:** 3935–3950

Xu X, Vreugdenhil D, van Lammeren AAM (1998) Cell division and cell enlargement during potato tuber formation. J Exp Bot **49:** 573–582

Yang W, Liu X, Zhang J, Feng J, Li C, Chen J (2010) Prediction and validation of conservative microRNAs of Solanum tuberosum L. Mol Biol Rep **37:** 3081–3087

Yoo BC, Kragler F, Varkonyi-Gasic E, Haywood V, Archer-Evans S, Lee YM, Lough TJ, Lucas WJ (2004) A systemic small RNA signaling system in plants. Plant Cell **16:** 1979–2000

Yu YY, Lashbrook CC, Hannapel DJ (2007) Tissue integrity and RNA quality of laser microdissected phloem of potato. Planta **226:** 797–803

Zhang H, Jin J, Tang L, Zhao Y, Gu X, Gao G, Luo J (2011a) PlantTFDB 2.0: update and improvement of the comprehensive plant transcription factor database. Nucleic Acids Res **39:** D1114–D1117

Zhang W, Luo Y, Gong X, Zeng W, Li S (2009) Computational identification of 48 potato microRNAs and their targets. Comput Biol Chem **33:** 84–93

Zhang X, Zou Z, Zhang J, Zhang Y, Han Q, Hu T, Xu X, Liu H, Li H, Ye Z (2011b) Over-expression of sly-miR156a in tomato results in multiple vegetative and reproductive trait alterations and partial phenocopy of the sft mutant. FEBS Lett **585:** 435–439

Zuker M (2003) MFold web server for nucleic acid folding and hybridization prediction. Nucleic Acids Res **31:** 3406–3415